

MEAN SUBTRACTION AND MODE SELECTION IN DYNAMIC MODE DECOMPOSITION

GOWTHAM S SEENIVASAHARAGAVAN*, MILAN KORDA†, HASSAN ARBABI ‡, AND IGOR MEZIĆ§

Abstract.

Koopman mode analysis has provided a framework for analysis of nonlinear phenomena across a plethora of fields. Its numerical implementation via Dynamic Mode Decomposition (DMD) has been extensively deployed and improved upon over the last decade. We address the problems of mean subtraction and DMD mode selection in the context of finite dimensional Koopman invariant subspaces.

Preprocessing of data by subtraction of the temporal mean of a time series has been a point of contention in companion matrix-based DMD. This stems from the potential of said preprocessing to render DMD equivalent to temporal DFT. We prove that this equivalence is impossible when the order of the DMD-based representation of the dynamics exceeds the dimension of the system. Moreover, this parity of DMD and DFT is mostly indicative of an inadequacy of data, in the sense that the number of snapshots taken is not enough to represent the true dynamics of the system.

We then vindicate the practice of pruning DMD eigenvalues based on the norm of the respective modes. Once a minimum number of time delays has been taken, DMD eigenvalues corresponding to DMD modes with low norm are shown to be spurious, and hence must be discarded. When dealing with mean-subtracted data, the above criterion for detecting synthetic eigenvalues can be applied after additional pre-processing. This takes the form of an eigenvalue constraint on Companion DMD, or yet another time delay.

Key words. Koopman operator, Mean subtraction, Dynamic Mode Decomposition, Spurious eigenvalues

AMS subject classifications. 37M10, 37N10, 47N20

1. Introduction. Operator theoretic approaches to analysing dynamical systems [14] saw a resurgence at the turn of the century [25, 9]. This has created a vibrant field of research over the past decade, riding the tide of the data revolution. The ideas involved balance reductionism and interpretability, and are backed by strong theoretical guarantees. Here, we focus on the Koopman (composition) operator which acts on functions/observables defined on the state space. This linear operator can capture all the richness of a dynamical system owing to its infinite dimensional nature. Furthermore, linearity permits the wealth of tools developed for linear systems [12] to be brought to their nonlinear counterparts [15].

A popular algorithm to approximate the action of the Koopman operator on a specified set of functions (dictionary) is the Dynamic Mode Decomposition (DMD) [29, 32, 34]. DMD finds the best finite dimensional matrix that propagates measurements one time step forward in a least squares sense. Leveraging the closure of functions under composition, Extended DMD (EDMD) then tries to find approximations that are more pertinent to the system at hand. Regardless, this approach can provably converge to the true Koopman operator. In particular, EDMD may exhibit convergence along sub-sequences [16], whereas endowing DMD data with a Hankel structure brings about convergence in the pseudo-spectral sense [1]. Hence, the spectral decomposition of the DMD matrix yields approximations to spectral objects of

*Department of Mechanical Engineering, University of California Santa Barbara

†Methods and Algorithms for Control, LAAS-CNRS

‡Department of Mechanical Engineering, Massachusetts Institute of Technology

§Department of Mechanical Engineering, University of California Santa Barbara

the composition operator. The right eigenvectors are called Koopman modes, and are used to decompose data into components that evolve exponentially in time. The left eigenvectors can be used to find Koopman eigenfunctions [34], which generalize the notion of invariants from classical mechanics [23]. Notice that the key is to work with functions on the state space, and not the states themselves. Here, we analyse the issues of mean subtraction and mode selection in DMD.

Mean subtraction is a preprocessing step shared by many learning algorithms. The Koopman mode decomposition (KMD) contains the long term time average as the first term [22], and its removal means that the residual signal has mean zero. This allows focus on temporally varying parts of the process, and has been adopted in a diverse set of analyses [5, 28, 31, 4]. Nonetheless, this step may render Companion DMD [29] equivalent to a temporal Discrete Fourier Transform (DFT) [7]. The unsettling consequences include misrepresentation of dissipative dynamics and a bijection between the trajectory length and DMD spectrum. A recent work [13] points out that [7] provides only a sufficient condition for such a reduction. Moreover, it is shown that these criteria are void when there is an underlying Koopman invariant subspace and more samples than its dimension. Here, we complete this line of thought and show that over-sampling is sufficient to negate this equivalence. In addition, an appropriate number of time delays [6, 1] ensures that taking enough samples is necessary for the non-equivalence of DMD and DFT.

Increasing the order of a DMD model *could* help describe rich dynamical behavior [17]. A setback with this approach is the deluge of DMD eigenvalues to contend with. A common choice is to neglect those corresponding to DMD modes with very small norm [29, 33, 2, 18, 11, 10]. We justify this choice by establishing a 1-1 correspondence between DMD modes of negligible norm and DMD eigenvalues that are numerical artifacts. This strategy can be used with mean-subtracted data too, provided the data is then delayed once or a DMD eigenvalue is constrained to be 1. These results rely upon using Koopman invariant observables and access to enough data. While former can be met with time delays, a partial answer to the latter can be obtained purely from data using endemic results on DMD-DFT equivalence.

This paper is organized as follows: [Section 2](#) details the notation adopted in this work. [Section 3](#) reviews some theoretical aspects of the Koopman operator, Dynamic Mode Decomposition and the effect of removing the temporal mean. Drawing on these, [Section 4](#) explores the relationship between mean subtracted DMD and DFT, resulting in an a posteriori check that alerts to data insufficiency. [Section 5](#) justifies DMD mode norm as a criterion for filtering out DMD eigenvalues using connections between matrix-vector operations and uni-variate polynomials. [Section 6](#) sees the numerical verification of all major results on a couple of linear time invariant systems (LTIs), the Van Der Pol oscillator and the lid-driven cavity at various flow regimes. This necessitates the development of computationally tractable versions of the theorems under scrutiny, and an algorithm that can select common eigenvalues arising from Companion DMD on multiple high-dimensional time traces. [Section 7](#) summarizes the findings and points out relevant questions that remain unanswered.

2. Notation. The notation for this work is fairly standard. Sets are denoted by $\{\}$ while vectors and matrices are enclosed by $[\]$. Index notation lends itself to the pervasive linear algebraic bent. A few oddities exist out of necessity, and we hope that skimming their specifics does not impede comprehension greatly.

2.1. Sets.

- Index notation:

$$\{\lambda_i\}_{i=1}^r = \{\lambda_1, \lambda_2, \dots, \lambda_r\}$$

- $\#(A) :=$ Cardinality of the set A .
- $\wp(A) :=$ Power set of A .
- Special sets:

$\mathbb{N} :=$ All natural numbers

$\mathbb{W} := \mathbb{N} \cup \{0\}$

(All whole numbers)

$\mathbb{C}_\infty := \cup_{j=1}^\infty \mathbb{C}^j$

(All finite dimensional vectors)

$\mathbb{C}_{\infty \times \infty} := \cup_{i=1}^\infty \cup_{j=1}^\infty \mathbb{C}^{i \times j}$

(All finite dimensional matrices)

2.2. Matrix-vector operations. Vectors are typically in \mathbb{C}^m , labelled with lower-case letters and represented as columns. Matrices are in $\mathbb{C}^{m \times n}$, denoted by upper-case letters and written as ordered sets of columns.

- Components (Columns) of a vector(matrix) are numbered from 1.
- Index notation:
 - Vectors

$$v = [v_i]_{i=1}^m = \begin{bmatrix} v_1 \\ v_2 \\ \vdots \\ v_m \end{bmatrix} \quad \emptyset =: [v_i]_{i=1}^0$$

- Matrices

$$A = [a_j]_{j=1}^n = [a_{ij}]_{i,j=1}^{m,n} = \begin{bmatrix} | & | & \cdots & | \\ a_1 & a_2 & \cdots & a_n \\ | & | & \cdots & | \end{bmatrix}$$

- e_i denotes the i -th standard basis vector.

$$\begin{aligned} I_n &= [e_j]_{j=1}^n \\ &=: [\delta_{ij}]_{i,j=1}^n \end{aligned}$$

- Special vectors and matrices

- Constant vectors and matrices are written as bold-faced symbols with their dimension as a subscript.

$$\begin{aligned} \mathbf{1}_m &= [1]_{i=1}^m \\ \mathbf{0}_{m \times n} &= [\mathbf{0}_m]_{j=1}^n = [0]_{i,j=1}^{m,n} \end{aligned}$$

- $\text{gp}_{n+1}[\lambda]$: First $n + 1$ terms of the geometric sequence beginning at 1 with ratio λ .

$$\text{gp}_{n+1}[\lambda] := [\lambda^{i-1}]_{i=1}^{n+1}$$

- $T[c]$: Companion matrix with 1 on the first sub-diagonal and c as the last column.

$$(T[c])_{i,j=1}^{\#[c]} := \begin{cases} c_i & j = \#[c] \\ \delta_{(i-1)j} & \text{Otherwise} \end{cases}$$

– $\mathcal{F}[n]$: DFT matrix of size n .

$$(2.1) \quad \begin{aligned} \omega[n] &:= e^{[i\frac{2\pi}{n}]} \\ \mathcal{F}[n] &:= \left[\frac{(\omega[n])^{-(j-1)(i-1)}}{n} \right]_{i,j=1}^n \end{aligned}$$

• Classical subspaces:

$$\begin{aligned} \mathcal{R}(Z) &:= \text{Range of } Z \\ \mathcal{N}(Z) &:= \text{Null-space of } Z \end{aligned}$$

- A^H denotes the Hermitian transpose of A , and A^T represents the transpose of A .
- Using the standard inner product on \mathbb{C}^m ,
 - $\mathcal{P}_{\mathcal{W}}$ denotes the orthogonal projector onto the subspace \mathcal{W}
 - A^\dagger refers to the Moore-Penrose pseudo-inverse of A .

3. Preliminaries.

3.1. Koopman setup. Consider an autonomous discrete time dynamical system in \mathbb{R}^p

$$(3.1) \quad x^+ = \mathbb{T}(x), \quad x \in \mathbb{R}^p$$

\mathbb{T} can be used to define a Koopman operator, U , that acts on functions on the state-space: [14, 26]

$$(3.2) \quad \begin{aligned} U : \mathcal{H} &\rightarrow \mathcal{H} \\ U \circ \psi &:= \psi \circ \mathbb{T} \end{aligned}$$

The space under study, \mathcal{H} , is the discrete-time version of a recent construction [21]. We make the following assumptions:

- $\mathcal{D} \subset \mathbb{R}^p$ is compact and invariant under \mathbb{T} .
- $\mathcal{A} \subset \mathcal{D}$ is a global attractor of zero Lebesgue measure.
- μ is the physical invariant measure on \mathcal{A} such that $\mu(\mathcal{A}) = 1$.

In this setting, \mathcal{H} is constructed as follows:

$$(3.3) \quad \begin{aligned} \mathcal{H}_A &:= \left\{ f : \mathcal{D} \rightarrow \mathbb{C} \mid \int_{\mathcal{D}} |f|^2 d\mu < \infty \right\} \\ \tilde{\mathcal{H}}_B &:= \left\{ f : \mathcal{D} \rightarrow \mathbb{C} \mid f \text{ is } \mathcal{C}^0 \text{ \& } \forall \phi \in \mathcal{H}_A, \int_{\mathcal{D}} f \phi d\mu = 0 \right\} \\ \mathcal{H}_B &:= \tilde{\mathcal{H}}_B \cup \mathbf{1} \\ \mathcal{H} &:= \mathcal{H}_A \otimes \mathcal{H}_B \end{aligned}$$

\mathcal{H}_A is invariant under U . If $\mathcal{H}_A \otimes \bar{\mathcal{H}}_B$ is also invariant under U , then U can be written thus:

$$(3.4) \quad \begin{aligned} U &= \int_{(-\pi, \pi]} \int_{\mathbb{C}} \lambda e^{i\theta} dP_\lambda dP_\theta \\ \sigma(U) &= Cl \left[\left\{ z \in \mathbb{C} \mid z = \lambda e^{i\theta} \text{ where } e^{i\theta} \in \sigma(U|_{\mathcal{H}_A}) \text{ \& } \lambda \in \sigma(U|_{\mathcal{H}_B}) \right\} \right] \end{aligned}$$

Here, P_λ and \mathcal{P}_θ are projection valued spectral measures associated with the restriction of U to \mathcal{H}_A and \mathcal{H}_B respectively.

Although infinite dimensional, U is a linear operator. The spectral objects of U can provide significant insight into the dynamics of (3.1) [22]. To begin with, linearity allows the eigen-functions of U , ϕ_j , to describe the evolution of any function in their span.

$$(3.5) \quad \begin{aligned} \forall j, \quad (U \circ \phi_j)(x) &= \phi_j(\Upsilon(x)) = \lambda_j \phi_j(x) \\ \implies (U \circ \sum_j c_j \phi_j)(x) &= \sum_j c_j \lambda_j \phi_j(x) \end{aligned}$$

These intrinsic objects can also recover well-established geometric concepts such as stable/unstable/center manifolds [21] and isochrons [19], as well as define new ones like isostables [20].

3.2. Dynamic Mode Decomposition. Dynamic Mode Decomposition [29, 34] finds a finite section of U [24], with respect to a specified set of observables (dictionary) $\Psi := [\psi_i]_{i=1}^m$. This is accomplished by a straightforward linear regression ¹:

$$(3.6) \quad \begin{aligned} X_{(m \times n)} &:= [\Psi(x_j)]_{j=1}^n \\ Y_{(m \times n)} &:= [U\Psi(x_j)]_{j=1}^n = [\Psi(\Upsilon(x_j))]_{j=1}^n \\ A_{\text{DMD}} &:= \min_A \|AX - Y\|_F^2 \end{aligned}$$

When the samples are successive iterates along the same orbit, i.e. $\forall j, x_{j+1} = \Upsilon(x_j)$, a more concise representation of U is made possible by the temporal structure²:

$$(3.7) \quad \begin{aligned} Z &:= [\Psi(x_j)]_{j=1}^{n+1} \\ &= [X \quad | \quad z_{n+1}] \end{aligned}$$

In this vein, Companion DMD attempts to find the n -dimensional invariant subspace that best approximates the time series [29] and is defined thus:

$$(3.8) \quad \begin{aligned} c^* &: \mathbb{C}_{\infty \times \infty} \rightarrow \mathbb{C}_{\infty} \\ c^*[Z] &:= \min_c \|Xc - z_{n+1}\|_2 \\ &= X^\dagger z_{n+1} \\ T^* &:= T[c^*[Z]] \end{aligned}$$

The Companion matrix T^* represents the aforementioned subspace. The spectral decomposition of T^* can be used to perform a Koopman mode decomposition of Z . Suppose T^* has distinct eigenvalues, i.e. $\sigma(T^*) = \{\lambda_i^*\}_{i=1}^n$. Let $v_\lambda^*(w_\lambda^*)$ denote the right(left) eigenvector for the corresponding $\lambda \in \sigma(T^*)$. Say V^* is the matrix of right eigenvectors that diagonalizes T^* into Λ^* , i.e. $T^* = V^* \Lambda^* (V^*)^{-1}$. It can be shown that $(V^*)^{-1} = [(\lambda_i^*)^{j-1}]_{i,j=1}^n$, which is a Vandermonde matrix. X and Y are then related as follows:

$$(3.9) \quad \begin{aligned} r^* &:= z_{n+1} - Xc^*[Z] \\ Y &= XT^* + r^* e_n^H \\ &= XV^* \Lambda^* (V^*)^{-1} + r^* e_n^H \quad (3.8) \\ &= D^* \Lambda^* (V^*)^{-1} + r^* e_n^H \quad (D^* := XV^*) \end{aligned}$$

¹Although it had been implicit since [29, 32], (3.6) was explicitly stated in [34] as Extended DMD.

²By Section 2, z_j denotes the j -th column of Z .

where r^* is the residual in Companion DMD (3.8). The columns of D^* , d_j^* , are termed DMD modes while λ_j^* are DMD eigenvalues. (3.9) now gives the following expansion:

$$(3.10) \quad \begin{aligned} z_i &= \sum_{j=1}^n d_j^* (\lambda_j^*)^{i-1}, \quad (r^*)^H z_i = 0 \quad i = 1, \dots, n \\ z_{n+1} &= \sum_{j=1}^n d_j^* (\lambda_j^*)^n + r^* \end{aligned}$$

Comparing the Koopman mode expansion [26] and (3.10) suggests that the DMD mode Xv_λ^* may approximate the Koopman mode corresponding to the eigenvalue λ^* . Further discussion on this topic can be found in [24].

3.3. Effect of mean subtraction. Mean subtraction is a useful pre-processing step when the time series, Z , is generated by the solution to a PDE with Dirichlet boundary conditions (BCs) [7]. It ensures that DMD based predictions using mean-subtracted data respect the BCs. This section summarizes relevant work on the potential drawback of this idea and efforts at resolution.

Let μ be the temporal mean of the time series.

$$\mu = \frac{1}{n+1} \left(\sum_{i=1}^{n+1} z_i \right) = \frac{1}{n+1} (Z \text{gp}_{n+1}[1])$$

Removing the mean from each snapshot gives mean-subtracted versions of Z and X :

$$(3.11) \quad \begin{aligned} Z_{ms} &:= [z_j - \mu]_{j=1}^{n+1} \\ X_{ms} &:= [z_j - \mu]_{j=1}^n \end{aligned}$$

Companion DMD on the mean subtracted data would then read:

$$(3.12) \quad \begin{aligned} c_{ms} &:= c^* [Z_{ms}] \\ &= X_{ms}^\dagger (z_{n+1} - \mu) \\ T_{ms} &:= T[c_{ms}] \end{aligned}$$

Under some conditions, it was shown that (3.12) is equivalent to a DFT on (3.11). This can be paraphrased using a set valued mapping, Δ^3 , that finds all possible candidates to (3.10):

$$(3.13) \quad \begin{aligned} \Delta : \mathbb{C}^{m \times (n+1)} &\rightarrow \wp(\mathbb{C}^{m \times n} \times \mathbb{C}^{n \times 1}) \\ \Delta(Z) &:= \text{All pairs } ([v_j]_{j=1}^n, [\lambda_j]_{j=1}^n) \text{ simultaneously satisfying} \\ &\begin{cases} \forall i \neq j, \lambda_i \neq \lambda_j \\ \forall i < n+1, z_i = \sum_{j=1}^n v_j \lambda_j^{i-1} \\ \forall i < n+1, (z_{n+1} - \sum_{j=1}^n v_j \lambda_j^n)^H z_i = 0 \end{cases} \end{aligned}$$

For example, suppose $z_i = \lambda^{i-1}$ for some $\lambda \neq 0$. Then, every pair of the form $(e_1^H, \lambda e_1^H + \sum_{j=2}^n v_j e_j^H)$ is contained in $\Delta(Z)$. Here, $\{v_j\}_{j=2}^n$ is any set of $n-1$ distinct complex numbers not equal to λ .

³It is crucial that each pair contains $n < n+1$ entries for a trajectory of length $n+1$. Any more, and every set of distinct complex numbers can be used to construct an element of Δ .

It is known that distinct DMD eigenvalues⁴ ensure $(XV^*, [\lambda_j^*]_{j=1}^n) \in \Delta(Z)$ [29]. In addition, if X has full column rank, Δ finds a unique mode-rate pair.

THEOREM 3.1. [7] *Let the eigen-decomposition of T^* be $T^* = V^*\Lambda^*(V^*)^{-1}$. Then, the following statements are equivalent:*

Statement 1: X has full column rank & Λ^ is diagonal with distinct entries*

Statement 2: $\Delta(Z) = \{(XV^, [\lambda_j^*]_{j=1}^n)\}$*

The utility of this result, seen in [Theorem 3.3](#), is that modes can be guessed if the first set of conditions hold. The equivalence of mean-subtracted DMD (abbreviated hereafter as μ DMD) with temporal DFT can now be explicitly defined:

- Complete equivalence (μ DMD \equiv DFT)

$$(3.14) \quad \begin{aligned} \Delta(Z_{ms}) &= \{(V_F, \Lambda_F)\} \\ V_F &:= [(Z_{ms}\mathcal{F}[n+1])_i]_{i=2}^{n+1} \\ \Lambda_F &:= [\omega[n+1]^i]_{i=1}^n \end{aligned}$$

- Spectral equivalence

$$(3.15) \quad c_{ms} = -\mathbf{1}_n \iff \exists(\hat{V}, \hat{\Lambda}) \in \Delta(Z_{ms}) \text{ such that } \hat{\Lambda} = \Lambda_F$$

Evidently, (3.14) \implies (3.15). The latter is easier to check and, indeed, is guaranteed if X_{ms} has linearly independent columns.

LEMMA 3.2. [7]

$$X_{ms} \text{ is full column rank} \implies c_{ms} = -\mathbf{1}_n$$

When the time-series has full column rank, the DMD eigenvalues and modes corresponding to (3.12) can be found by a temporal DFT on Z_{ms} .

THEOREM 3.3. [7]

$$Z \text{ has full column rank} \implies \mu\text{DMD} \equiv \text{DFT}$$

Proof.

$$\begin{aligned} &Z \text{ is full column rank} \\ \implies &X_{ms} \text{ is full column rank} \\ \implies &c_{ms} = -\mathbf{1}_n \quad (\text{Lemma 3.2}) \\ \implies &\Delta(Z_{ms}) \text{ has a single element} \quad (\text{Theorem 3.1}) \end{aligned}$$

Post multiplying Z_{ms} by $\mathcal{F}\mathcal{F}^{-1}$, one gets the desired conclusion⁵. \square

Note that [Theorem 3.3](#) is a sufficiency condition. A crucial step is that X_{ms} be full column rank. This does not hold under assumptions that are tantamount to the simultaneous existence of the following [13] :

- A finite dimensional Koopman invariant subspace that contains Ψ
- A trajectory that is *long enough*.
- A DMD eigenvalue at 1
- Non-zero mean.

The first assumption induces a lot of structure that merits a closer look.

⁴and hence T^* is diagonalizable

⁵The value of c_{ms} informs calling on \mathcal{F} .

3.3.1. Finite dimensional Koopman invariant subspaces. Let $\Psi = [\psi_i]_{i=1}^m$, the vector of m observables, lie in a r -dimensional invariant subspace \mathcal{V} of U . Suppose $U|_{\mathcal{V}}$ has r -distinct eigenvalue-eigenfunction pairs: $\{(\lambda_j, \phi_j)\}_{j=1}^r$. If $\Lambda := [\lambda_i \delta_{ij}]_{i,j=1}^r$, we have the following:

$$\begin{aligned}\mathcal{V} &= \text{span}(\{\phi_i\}_{i=1}^r) \\ \sigma(\Lambda) &= \{\lambda_j\}_{j=1}^r\end{aligned}$$

Note that Λ is the representation of $U|_{\mathcal{V}}$ using $\{\phi_j\}_{j=1}^r$. With $\Phi := [\phi_j]_{j=1}^r$, we can write:

$$(3.16) \quad \begin{aligned}\Phi^+ &:= U\Phi = \Lambda\Phi \\ \Psi &=: \tilde{C}\Phi\end{aligned}$$

We now define C as the column scaling of \tilde{C} by the eigen-coordinates of x_1 .

$$(3.17) \quad C := \tilde{C}[\phi_i(x_1)\delta_{ij}]$$

Without loss of generality, we assume that every column of \tilde{C} is non-zero and that $\phi_i(x_1) \neq 0, \forall i = 1, \dots, r$. Hence, every column of C is also non-zero. These permit a compact representation of the time series Z ⁶:

$$(3.18) \quad \begin{aligned}\Theta &:= [(\lambda_i)^{j-1}]_{i,j=1}^{r,n+1} \\ Z &= [z_j]_{j=1}^{n+1} \\ &= C\Theta\end{aligned}$$

Here, Θ is a Vandermonde matrix constructed using $\sigma(\Lambda)$. Consequently, it is also seen in many derived quantities.

$$\begin{aligned}X &= [z_j]_{j=1}^n =: C\Theta_1 \\ Y &= [z_i]_{i=2}^{n+1} = C\Lambda\Theta_1\end{aligned}$$

Now, suppose the eigenvalues of Λ are arranged in the order of decreasing magnitude. Further, let q^* be the number of non-zero eigenvalues of Λ .⁷

THEOREM 3.4. [13] *Suppose the following hold simultaneously:*

- *Either $n \geq q^* + 1$ or $n \geq q^*$ & $\mathcal{R}(X) = \mathcal{R}(Y)$*
- *YX^\dagger has an eigenvalue at 1*
- *$\mu \neq 0$*

Then, $\text{rank}(X_{ms}) \leq \text{rank}(X) - 1$

While this sheds some light on the issue of mean subtraction, it must be noted that the rank condition on X_{ms} was *only* proven sufficient in [Lemma 3.2](#).

4. Charting the domain of DMD-DFT equivalence. We begin with a necessary and sufficient condition for the spectral equivalence of DMD and DFT (3.15).

THEOREM 4.1. *Spectral equivalence to temporal DFT holds iff the constant vector is orthogonal to $\mathcal{N}(X_{ms})$.*

$$\mathcal{P}_{\mathcal{N}(X_{ms})}\mathbf{1}_n = 0 \iff c_{ms} = -\mathbf{1}_n$$

⁶Details in [Appendix B.1](#)

⁷Hence, $r \leq q^* + 1$

Proof. Refer [Appendix B.2](#) □

Thus, the search for parameter regimes (if they exist) when (3.15) is void can be safely redirected to find situations where $\mathcal{P}_{\mathcal{N}(X_{m_s})}\mathbf{1}_n \neq 0$. A potential lead suggested by [Theorem 3.4](#) is to take a sufficiently large number of snapshots. Before proceeding further, we categorize the relation between n and r into 3 sampling regimes.

When $n < r$, T^* cannot capture all r eigenvalues and so the data is said to be under-sampled. $n = r$ is just-sampled as it permits all eigenvalues to be accounted for, while $n > r$ is over-sampled.

We now show that over-sampling removes the equivalence of mean-subtracted DMD and DFT.

THEOREM 4.2. *Mean-subtracted DMD is not a temporal DFT when over-sampled.*

$$n \geq r + 1 \implies c_{ms} \neq -\mathbf{1}_n$$

Proof. Refer [Appendix B.2](#) □

Thus, [Theorem 3.4](#) is extended by merely holding onto the assumption on trajectory length. The contrapositive is of practical interest: Equivalence of mean-subtracted DMD and DFT signals a need to acquire more data for a reliable analysis. When the span of the observables (Ψ) contains the underlying Koopman invariant subspace (\mathcal{V}), the remaining data regimes can be scrutinized:

COROLLARY 4.3. *\tilde{C} is full column rank.*

- $n = r : \mu\text{DMD} \equiv \text{DFT} \iff 1 \notin \sigma(A)$
- $n < r \implies \mu\text{DMD} \equiv \text{DFT}$

Proof. Refer [Appendix B.2](#) □

Thus, we have a complete understanding of DMD-DFT equivalence, as defined in (3.14) and (3.15), when the observables span a Koopman invariant subspace. Barring the pragmatically negligible case of just-sampling ($n = r$), under-sampling is necessary and sufficient for the equivalence of DMD and DFT. A vital ingredient to drawing these conclusions is the Koopman invariance of Ψ , which is equivalent to the left-invertibility of \tilde{C} . While this may not always hold, one remedy is to time delay the data $r - 1$ times, assuming one has enough snapshots at hand.

COROLLARY 4.4. *Suppose we can access observables, Υ , defined thus:*

$$\Upsilon := C_0\Phi$$

Without loss of generality, all columns of C_0 are non-zero.

If Ψ is generated from Υ by taking $r - 1$ delays, then \tilde{C} has full column rank. In other words,

$$\Psi = \begin{bmatrix} \Upsilon \\ \Upsilon \circ T \\ \vdots \\ \Upsilon \circ T^{r-1} \end{bmatrix} \implies \tilde{C} \text{ has full column rank}$$

Proof. By construction, we have

$$\tilde{C} = \begin{bmatrix} C_0 \\ C_0\Lambda \\ C_0\Lambda^2 \\ \vdots \\ C_0\Lambda^{r-1} \end{bmatrix}$$

The right eigenvectors of Λ are the standard basis vectors and no column of C_0 is 0. Hence, by the Eigenvector test for Observability [12], (Λ, C_0) is an observable pair. Since \tilde{C} is the observability Grammian of (Λ, C_0) , it has full column rank. \square

In short, oversampling always precludes the equivalence of mean-subtracted DMD and DFT. Consequently, DMD produces accurate results with sufficiently long samples, larger than the dimension of the underlying Koopman invariant subspace. The converse holds when the observables used are Koopman invariant and this can be attained by delay embedding the snapshots.

5. Extracting invariant subspaces. Non-equivalence of mean-subtracted DMD and DFT beyond a certain trajectory length, persistent across a range of delays, *could* indicate an invariant subspace that contains the chosen observables. However, this transition is often smoothed over a range of snapshots⁸ and only results in the demarcation of a *subset* of the over-sampled regime. In this data-rich regime, if the observables are Koopman invariant, we show that the DMD eigenvalues ($\sigma(T^*)$) contain the true Koopman eigenvalues ($\sigma(\Lambda)$). Furthermore, the corresponding Koopman modes are the only non-zero DMD modes.

The overarching proof strategy is to represent operations on uni-variate polynomials using matrix-vector products [30, 8]. A discussion of these ideas in the context of this work can be found in [Appendix C](#). The proofs of the mode-extraction theorems below often begin with a parametrization of polynomials whose roots contain the desired Koopman eigenvalues. The onus is, then, to show that the DMD mode norm can sift the roots of the polynomial singled out by the pertinent minimization.

5.1. Spectral objects without mean-subtraction. We now formally define the set of “DMD eigenvalues with non-trivial DMD modes”:

$$\sigma_{nontriv}[Z, c] := \{\lambda \in \sigma(T[c]) \mid \exists v_\lambda \text{ such that } T[c]v_\lambda = \lambda v_\lambda \ \& \ Xv_\lambda \neq 0\}$$

This permits a succinct exposition of the elucidating nature of DMD mode norms. We present a relatively abstract formulation, that is then specialized to cases with and without mean subtraction.

THEOREM 5.1. *Let $\check{C} \in \mathbb{C}^{m \times r}$. Define:*

$$\check{c}^* := c^*[\check{C}\Theta], \quad \check{T}^* := T[\check{c}^*]$$

Then,

$$\check{C} \text{ is full column rank} \ \& \ n \geq r \implies \sigma_{nontriv}[\check{C}\Theta, c^*(\check{C}\Theta)] = \sigma(\Lambda)$$

Proof. Refer [Appendix D](#) \square

⁸See [Figure 6.1](#) for numerical evidence

In order to study Z , (3.18) suggests C presume the role of \tilde{C} in Theorem 5.1. A closer look shows that the rank-requirement can be relegated to the more intrinsic quantity \tilde{C} .

COROLLARY 5.2.

$$\tilde{C} \text{ is full column rank} \quad \& \quad n \geq r \implies \sigma_{\text{nontriv}}[Z, c^*(Z)] = \sigma(\Lambda)$$

Proof. By (3.17), \tilde{C} is full column rank $\implies C$ has full column rank. Apply Theorem 5.1 with $\tilde{C} \rightarrow C$. \square

Therefore, when the span of Ψ contains Φ , Companion DMD on a trajectory of length greater than the dimension of the underlying subspace ($n + 1 > r$) can coherently extract $\sigma(\Lambda)$. The condition on Ψ can be met by taking enough delays, as shown in Corollary 4.4. Consequently, a trajectory of length $2r$ is sufficient to characterize an r -dimensional Koopman invariant subspace.

5.2. Spectral objects with mean-subtraction. We now detail strategies to extract $\sigma(\Lambda)$ from mean-subtracted data. Here, mean is defined in a more general sense, i.e:

$$(5.1) \quad \mu_\lambda := \frac{1}{n+1} \left(\sum_{i=1}^{n+1} z_i \lambda^{-(i-1)} \right) = \frac{1}{n+1} (Z_{\text{gp}_{n+1}}[\lambda^{-1}])$$

The corresponding mean-subtracted data-sets are:

$$(5.2) \quad Z_{ms}^\lambda := [z_i - \mu_\lambda \lambda^{i-1}]_{i=1}^{n+1}, \quad X_{ms}^\lambda := [z_i - \mu_\lambda \lambda^{i-1}]_{i=1}^n, \quad Y_{ms}^\lambda := [z_i - \mu_\lambda \lambda^{i-1}]_{i=2}^{n+1}$$

This would correspond to a single step of Generalized Laplace Analysis (GLA) [23, 27] on Z if λ were the Koopman eigenvalue with the largest magnitude in the corresponding KMD. It also coincides with the setting in the later part of [13]. Note that there are two distinct relations possible between λ and $\sigma(\Lambda)$.

$$(5.3) \quad \begin{aligned} \text{Case 1: } & \sigma(\Lambda) \subset \lambda \{\omega[n+1]^j\}_{j=1}^{n+1} \quad (n - \text{periodic wrt } \lambda) \\ \text{Case 2: } & \sigma(\Lambda) \not\subset \lambda \{\omega[n+1]^j\}_{j=1}^{n+1} \end{aligned}$$

Case 1 is well-structured, in that $\sigma(\Lambda)$ is a subset of the $(n+1)$ -th roots of unity, scaled by λ . Hence, the Koopman eigenvalues lie on the circle of radius $|\lambda|$, and the arc joining any pair subtends an integral multiple of $\frac{2\pi}{n+1}$. Additionally, this class can be handled without any pre-processing, as mean-subtraction does not “confound” the true spectrum.

However, Case 1, if observed, only occurs periodically with respect to the number of snapshots. As an example, consider $\lambda = 1$ and $\sigma(\Lambda) = \{-1, 1, i, -i\}$. By (5.3), Case 1 is observed *only* for $n = 4i + 3, i \in \mathbb{N}$. The $n + 1$ -th power of the eigenvalues does not coincide with 1 for the remaining values of n , and hence they are classified as Case 2. Unfortunately, the effect of mean subtraction is more nuanced in Case 2 and requires some diligent pre-processing.

For the remainder of this section, we make the following assumption, with an eye towards using Theorem 5.1:

$$(5.4) \quad r \geq 2 \quad \& \quad \tilde{C} \text{ has full column rank.}$$

5.2.1. Without pre-processing. When $\sigma(\Lambda)$ is n -periodic wrt λ , mean subtraction either deletes λ or leaves Z untouched. Formally,

THEOREM 5.3. *Suppose it is Case 1 in (5.3) and (5.4) holds. Then, we have*

$$n \geq r \implies \sigma_{\text{nontriv}}[Z_{ms}^\lambda, c^*(Z_{ms}^\lambda)] = \sigma(\Lambda) - \{\lambda\}$$

Proof. Refer [Appendix E.1](#) □

Although similar to [Corollary 5.2](#), the proof shows that when $\lambda \in \sigma(\Lambda)$, mean subtraction lowers the number of snapshots that suffice to $r - 1$.

[Theorem 5.3](#) can also clarify a subtle difference between DMD-DFT equivalence, as defined in (3.14) and (3.15), and the conventional interpretation of the phrase. Suppose C has full column rank, $\sigma(\Lambda) = \{1, -1, i, -i\}$, $\lambda = 1$ and $n = 7$. Since this is Case 1 and $r \geq 2$, [Lemma E.1](#) says mean subtraction simply deletes the mode corresponding to 1. Hence, a conventional DFT along time will produce prominent peaks at the other Koopman eigenvalues, which happen to be the other roots of unity at 4. In this context, it would seem that [Theorem 4.2](#) is contradictory since it proclaims a non-equivalence of DMD and DFT. Resolving this simply requires a closer look, which shows that $c_{ms} \neq -\mathbf{1}_n$ does not preclude $T[c^*(Z_{ms}^1)]$ from having $-1, i$ and $-i$ in its spectrum. In fact, [Theorem 5.3](#) guarantees that these three Koopman eigenvalues are exactly the DMD eigenvalues with non-zero modes.

5.2.2. With pre-processing. For Case 2 and $r \geq 2$, no standard basis vector (e_j) lies in the nullspace of $\text{pre}_{n+1}[\lambda]$. Hence, removing the mean does not simply delete the row corresponding to λ , even if it were present in Θ . Indeed, it exacerbates the situation by removing the Koopman invariance of Ψ given by (5.4). We discuss two simple pre-processors that put us back in familiar territory.

Preserve λ . Consider Companion DMD using Z_{ms}^λ with the additional requirement that λ be an eigenvalue of $T[c]$. [Lemma D.2](#) shows that this can be imposed as a linear constraint, giving rise to the following optimization routine.

$$(5.5) \quad \begin{aligned} c_{pres}^*[Z, \lambda] &:= \arg \min_c \|Xc - z_{n+1}\|_2^2 \\ &\text{subject to } gp_{n+1}[\lambda] \begin{bmatrix} c \\ -1 \end{bmatrix} = 0 \end{aligned}$$

Some quantities analogous to c^*, T^* are:

$$(5.6) \quad \begin{aligned} c_{\lambda, pres}^* &:= c_{pres}^*[Z_{ms}^\lambda, \lambda] \\ T_{\lambda, pres}^* &:= T[c_{\lambda, pres}^*] \\ v_{pres}^* &:= \text{Right-eigenvector of } T_{\lambda, pres}^* \end{aligned}$$

Restricting the search to Companion matrices that have λ as an eigenvalue allows us to sidestep the effect of mean subtraction. Hence, mode norm continues to delineate $\sigma(\Lambda)$, with or without λ as allowed by the case under purview.

THEOREM 5.4. *Suppose (5.4) holds. Then, we have:*

$$n \geq r + 1 \implies \sigma_{\text{nontriv}}[Z_{ms}^\lambda, c_{\lambda, pres}^*] = \begin{cases} \sigma(\Lambda) - \{\lambda\} & \text{Case 1} \\ \sigma(\Lambda) \cup \{\lambda\} & \text{Case 2} \end{cases}$$

Proof. Refer [Appendix E.2.1](#) □

Take a delay. A simpler idea, seen for instance in [4], is to analyse the data-set after a single delay i.e.:

$$Z_{ms,del}^\lambda := \begin{bmatrix} X_{ms}^\lambda \\ Y_{ms}^\lambda \end{bmatrix}$$

Companion DMD on the above yields some familiar quantities:

$$(5.7) \quad \begin{aligned} c_{\lambda,del}^* &:= c^*[Z_{ms,del}^\lambda] \\ T_{\lambda,del}^* &:= T[c_{\lambda,del}^*] \\ v_{del}^* &:= \text{Right-eigenvector of } T_{\lambda,del}^* \end{aligned}$$

In contrast to the earlier approach, taking a delay tackles the loss of Koopman invariance directly. One lifts the dictionary with a time delay, instead of restricting it, to get a Koopman invariant set of observables. The outcome, though, remains the same as [Theorem 5.4](#), save a minuscule increase in data requirements.

THEOREM 5.5. *Suppose (5.4) holds. Then, we have:*

$$\begin{aligned} \text{Case 1: } n \geq r + 1 &\implies \sigma_{nontriv}[Z_{ms,del}^\lambda, c_{\lambda,del}^*] = \sigma(\Lambda) - \{\lambda\} \\ \text{Case 2: } n \geq r + 2 &\implies \sigma_{nontriv}[Z_{ms,del}^\lambda, c_{\lambda,del}^*] = \sigma(\Lambda) \cup \{\lambda\} \end{aligned}$$

Proof. Refer [Appendix E.2.2](#) □

6. Numerical experiments. We study numerically observable consequences of the transient predictions in [Theorem 4.2](#) and [Corollary 4.3](#) & the spectral guarantees in [Corollary 5.2](#) and [Theorems 5.3](#) to [5.5](#). The aforementioned indicators are computed over a set of randomly chosen orbits, for a range of n and $\#[delays]$ (number of delays). The former is implicated in every major result, while the latter, according to [Corollary 4.4](#), is an established means of meeting the relevant sufficiency conditions. We test this methodology^{9 10} on LTI systems, the Van der Pol oscillator and the lid-driven cavity at various Reynolds numbers [3].

6.1. (Non)-equivalence of DMD and DFT. The RMS error between c_{ms} and $-\mathbf{1}_n$ can measure the deviation of mean-subtracted DMD from DFT.

$$(6.1) \quad \delta_{rel}^\mu[c_{ms}] := \frac{\|c_{ms} - (-\mathbf{1}_n)\|}{\sqrt{n}}$$

First, we analyse the linear time invariant systems resulting from the following simplifications to [\(3.1\)](#) and [\(3.16\)](#):

$$(6.2) \quad T_i(x) = \Lambda_i x, \quad \Phi_i(x) = x, \quad \Upsilon_i = C_{0,i} \Phi_i, \quad i = 1, 2$$

where $C_{0,i}$ are randomly generated row vectors with non-zero entries and Λ_i are diagonal matrices. Specifically, LTI_1 is neutrally stable with $\sigma(\Lambda_1) = \{e^{i\frac{2j\pi}{7}}\}_{j=1}^7$. In contrast, LTI_2 has eigenvalues on both sides of the unit circle: $\sigma(\Lambda_2)$ comprises of 7

⁹All code used in this analysis can found at https://github.com/gowtham-ss-ragavan/mselect_dmd.git

¹⁰A relative threshold of 10^{-8} is used in all pseudo-inverse computations. The reduced matrix will be indicated by the subscript “reduced”.

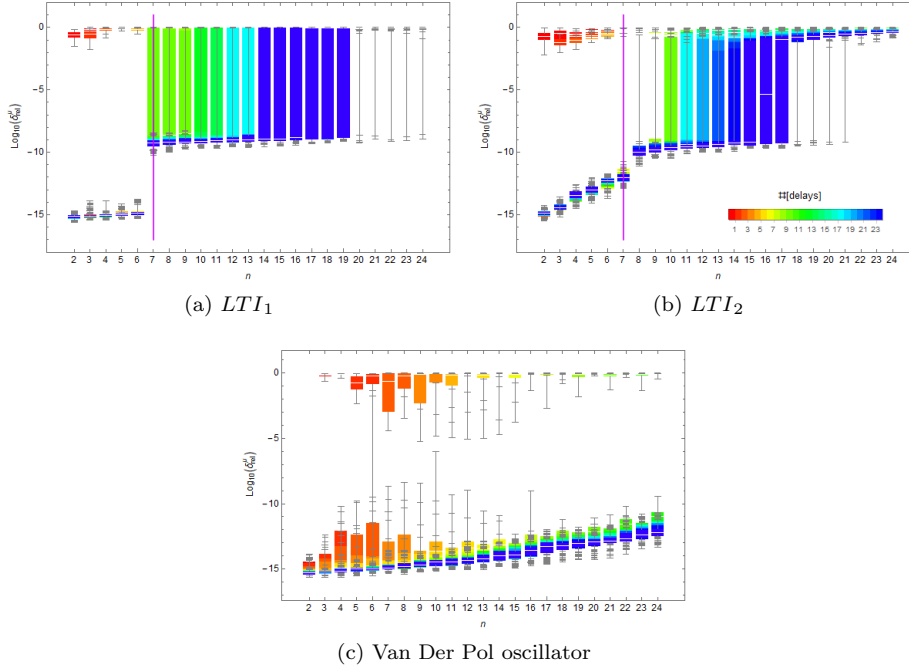


FIG. 6.1. Box plots of δ_{rel}^μ reveal its dependence on n and $\#[delays]$ (Colour-coded). Magenta line indicates r (when it is known). For $\#[delays] \geq 6$, $LTI_1(LTI_2)$ displays a persistent jump starting at $7(8)$ as predicted by [Theorem 4.2](#) and [Corollary 4.3](#). Such consistency is utterly lacking in the Van Der Pol oscillator, potentially indicating an invariant subspace of dimension greater than 23.

samples from a uniform distribution on the annulus of inner (outer) radius 0.8 (1.2) centred about the origin. In particular, $1 \notin \sigma(\Lambda_2)$.

Since every entry of $C_{0,i}$ is non-zero, $r = 7$ for both LTI_1 and LTI_2 . By [Corollary 4.4](#), $\#[delays] \geq 6$ will ensure that the corresponding \tilde{C} has full column rank. Hence, [Theorem 4.2](#) and [Corollary 4.3](#) say that if at-least 6 time delays are taken, the RMS error will be insignificant whenever $n < 7$, with a reversal beginning at $7(8)$ for $LTI_1(LTI_2)$. [Figure 6.1](#) goes beyond merely reflecting this trend: δ_{rel}^μ is orders of magnitude larger when n crosses the critical value. The shadowing of this trend by the pertinent inter-quartile ranges (IQRs), denoted by boxes coloured according to the number of delays taken, suggests that the observation is independent of the choice of initial condition. The icing on the cake is that when $n = r$, the effect of having $1 \in \sigma(\Lambda)$ is in concordance with [Corollary 4.3](#).

In contrast, the Van der Pol oscillator, described below, does not seem to have a low-dimensional invariant subspace:

$$\begin{aligned}
 x &:= [x_1 \quad x_2]^T \\
 \dot{x} &= [x_2 \quad (1 - x_1^2)x_2 - x_1]^T \\
 \Upsilon[x] &:= x
 \end{aligned}$$

Even though it also exhibits a step-like behaviour, increasing the number of delays pushes the discontinuity to larger n . By [Corollary 4.4](#), we can infer that the state variables do not lie a invariant subspace of dimension lower than 24.

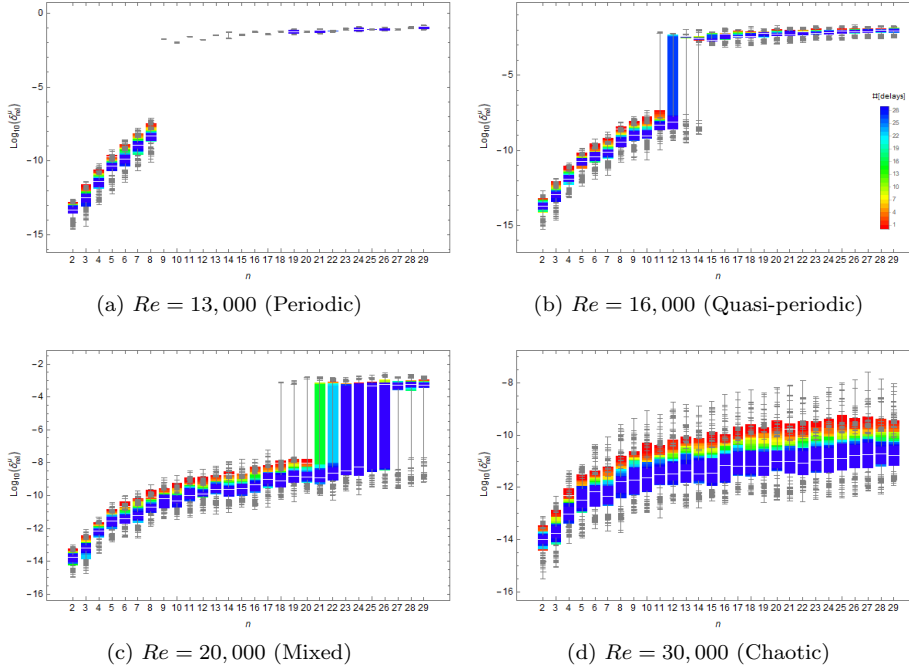


FIG. 6.2. Box plots of δ_{rel}^H delineate qualitatively different flow regimes. The first three display jumps robust to the number of delays, while the last is conspicuous in its lack of a discontinuity. These trends reflect the increasing complexity of the generating flow.

We close this discussion with the lid-driven cavity over a range of Reynolds numbers (Re). As Re increases, the flow transitions from periodic to chaotic, passing through quasi-periodic and mixed behaviour [3]. Here, the accessible observables, Υ , are samples of a stream-function at various grid-points. However, the underlying Koopman invariant subspace, if it exists, and the resultant C_0 are unknown. DMD-DFT transition offers a *potential* answer to this question. Figure 6.2 evinces the qualitative change in dynamics, over the range of Re , with an increasingly smoothed jump that shifts to larger values of n , eventually disappearing altogether. This alludes to the presence of a Koopman invariant subspace in all but the last case. Subsequently, in Subsection 6.2.2, we estimate these subspaces to check Corollary 5.2.

6.2. Mode-theorems. Testing the mode-extraction theorems (Corollary 5.2 and Theorems 5.3 to 5.5) requires information about the underlying system, namely Λ . This is known for LTI_1 and LTI_2 , and their analysis comprises the first section. Subsequently, we develop an algorithm to estimate Λ from a list of c^* , and thereby perform checks for relevant cavity flows.

6.2.1. Known subspace. The common theme of mode-extraction theorems is that they provide conditions that ensure the following:

$$(6.3) \quad \sigma_{nontriv}(Z, c) = B$$

Here, Z represents the data matrix, c the DMD optimum and B is derived from $\sigma(\Lambda)$ by including or excluding λ . Numerical verification of (6.3) requires two theoret-

ically sound but computationally absurd operations. At the highest level, we have a set equality while the search for non-zero DMD mode ensues one level below. Hence, we develop¹¹ two non-negative indicators, ρ_{subset} and $\delta_{trivial}$, whose equality to 0 is necessary and sufficient for (6.3). More precisely, for every mode-extraction theorem, using parameters as detailed in Table 6.1, the following holds:

$$\rho_{subset} = 0 \ \& \ \delta_{trivial} = 0 \iff (6.3)$$

Thus, low values of both indicators, under the specified conditions, would numerically vindicate the theorem being scrutinized.

TABLE 6.1
Parameters in (6.3) for mode-extraction theorems.

$B \setminus (Z, c)$	$(Z, c^*[Z])$	$(Z_{ms}^\lambda, c^*[Z_{ms}^\lambda])$	$(Z_{ms}^\lambda, c_{\lambda, pres}^*)$	$(Z_{ms, del}^\lambda, c_{\lambda, del}^*)$
Case 1	$\sigma(\Lambda)$	$\sigma(\Lambda) - \{\lambda\}$	$\sigma(\Lambda) - \{\lambda\}$ $B_0 = \sigma(\Lambda) \cup \{\lambda\}$	$\sigma(\Lambda) - \{\lambda\}$
Case 2	$\sigma(\Lambda)$	NA $(\sigma(\Lambda) \cup \{\lambda\})$	$\sigma(\Lambda) \cup \{\lambda\}$	$\sigma(\Lambda) \cup \{\lambda\}$

For both LTI systems under study, (5.4) can be met when $\#[delays] \geq 6$. Therefore, in the discussion that follows, the predicted trends will be checked only where this condition holds.

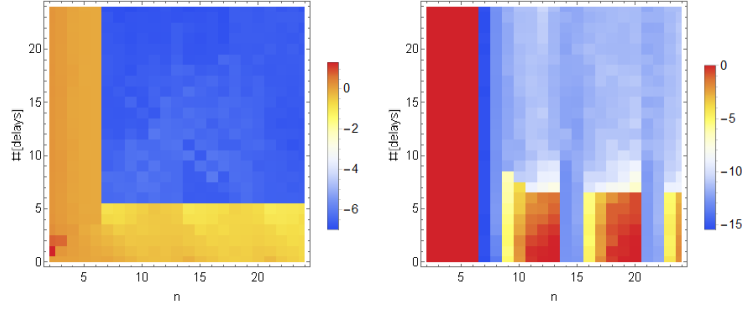
Corollary 5.2 applied to LTI_1 says that we should have both ρ_{subset} and $\delta_{trivial}$ drop to 0 for $n \geq 7$. This is evident in the first panel of Figure 6.3. Theorems 5.4 and 5.5 predict a similar trend for $n \geq 8$ and 9 respectively. Finally, note that Theorem 5.3 is only applicable for Case 1. This happens for LTI_1 when $n = 6, 13$ and 20. At these particular values, the second panel in Figure 6.3 appears to agree well with Theorem 5.3.

The analysis of LTI_2 is virtually the same. The difference arises in checking Theorem 5.3, which in fact does not apply for any value of n when $\lambda = 1$. It would seem that $\sigma(T[c_{ms}])$ tries to encompass $\sigma(\Lambda) \cup \{\lambda\}$ as n increases. But the accuracy is nowhere close to any of the other paths.

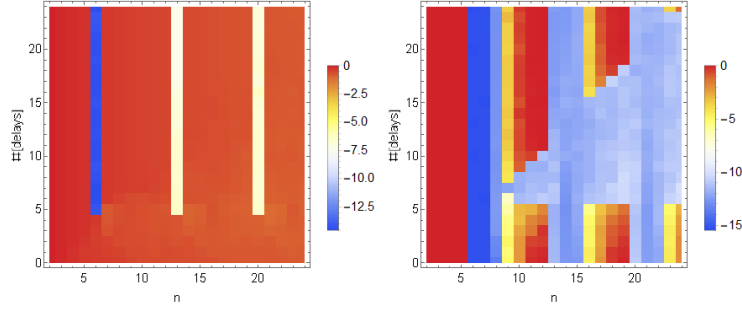
6.2.2. Unknown invariant subspace. The objective of this section is to check Corollary 5.2 for the cavity flows at Re 13, 16 and 20k. This necessitates a knowledge of $\sigma(\Lambda)$, the spectrum of the underlying Koopman invariant subspace. Theorem 4.2 and Corollaries 4.4 and 5.2 can be leveraged to this end, when we only have a single sequence of snapshots. The same tactic can also be adapted to multiple time traces by simply stacking the time series on top of each other. Alas, this can be prohibitive when the dictionary is gargantuan, as is often the case in fluid flows.

Algorithm 6.2 attempts to circumvent this issue with a divide-and-conquer approach. First, Companion DMD (3.8) and its mean-subtracted version (3.12) are performed on each trajectory, over the set of hyper-parameters that are accessible. Then, a lower bound (\hat{r}_{min}) and an upper bound (\hat{r}_{max}) on the possible values of r are found using Theorem 4.2 and Corollary 4.3. Now, for each valid model order \hat{r} , the DMD eigenvalues from all trajectories with sufficient delays (see Corollary 4.4) are assimilated using Algorithm 6.1. The essence of this sub-routine is the use of a weighted collection of the corresponding characteristic polynomials to estimate common eigenvalues via the SVD. Corollary 5.2 guarantees that common DMD eigenvalues will

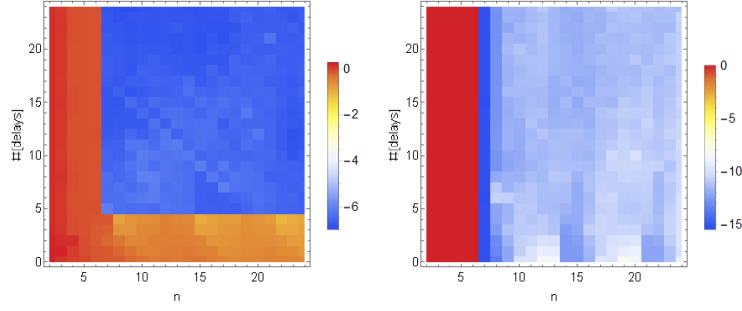
¹¹Details can be found in Appendix F.1



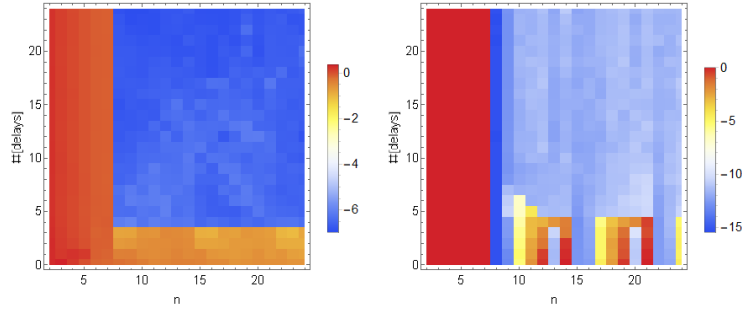
(a) Corollary 5.2



(b) Theorem 5.3

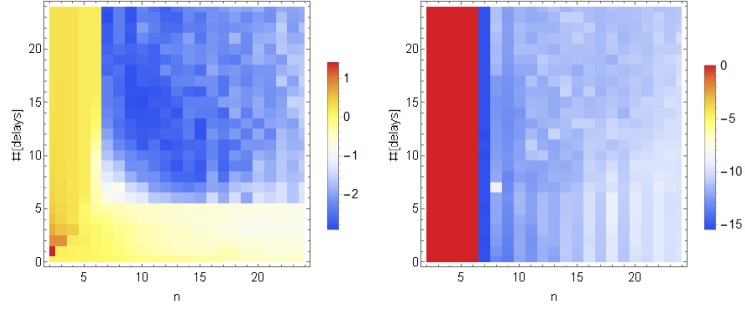


(c) Theorem 5.4

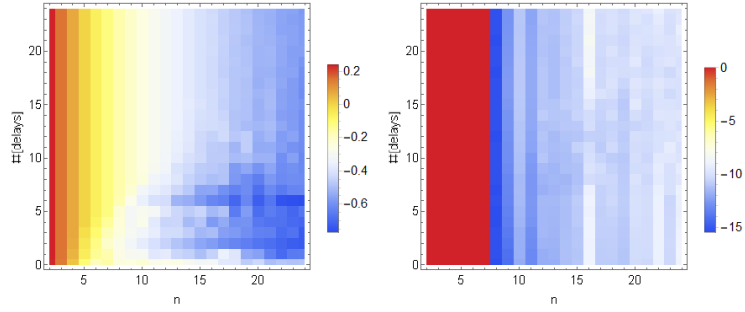


(d) Theorem 5.5

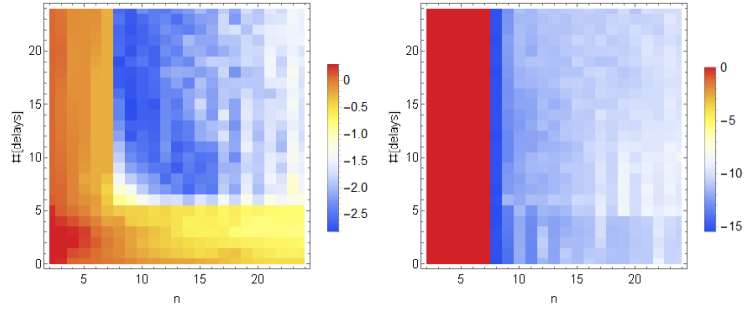
FIG. 6.3. Verifying the mode-extraction theorems for LTI_1 when $\lambda = 1$. The left (right) column shows the 95-th percentile of $\rho_{\text{subset}}(\delta_{\text{trivial}})$ on a \log_{10} scale, over 50 orbits. For $n \geq 7$ and $\#[\text{delays}] \geq 6$, both indicators drop to 0 as predicted. See discussion for (b)



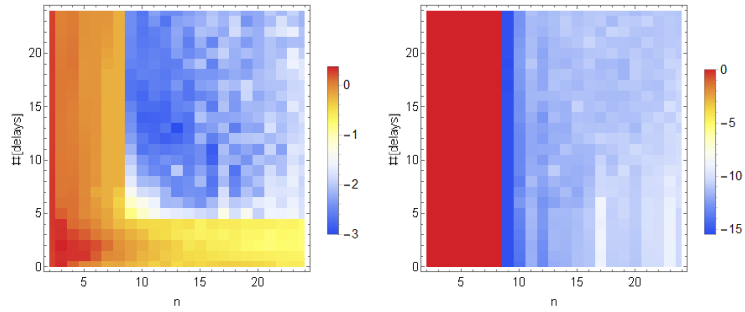
(a) Corollary 5.2



(b) Theorem 5.3



(c) Theorem 5.4



(d) Theorem 5.5

FIG. 6.4. Verifying the mode-extraction theorems for LTI_2 when $\lambda = 1$. The left (right) column shows the 95-th percentile of ρ_{subset} (δ_{trivial}) on a \log_{10} scale, over 50 orbits. For $n \geq 7$ and $\#[\text{delays}] \geq 6$, both indicators drop to 0 as predicted. See discussion for (b)

contain all the Koopman eigenvalues. Therefore, a residual criterion is then used to pick \hat{r} common eigenvalues¹². The parent algorithm culminates with the selection of a model order whose corresponding eigenvalues are best subsumed by the higher order versions.

Algorithm 6.1 Collecting DMD eigenvalues common to multiple analyses

- 1: Inputs: Results of Companion DMD of order \hat{n} on N trajectories $\{c_i\}_{i=1}^N$, weights $\{w_i\}_{i=1}^N$ and a number $\hat{r} \leq \hat{n}$.
 - 2: $W := [w_i \delta_{ij}]_{i,j=1}^N$, $A := \begin{bmatrix} c_i \\ -1 \end{bmatrix}_{i=1}^N$
 - 3: Compute u_1 , the dominant left singular vector of AW
 - 4: $\hat{\nu} :=$ roots of $\text{gp}_{\hat{n}+1}[\nu]^T u_1$, a polynomial in ν of degree \hat{n} .
 - 5: $\nu :=$ Elements of $\hat{\nu}$ corresponding to the \hat{r} -lowest values of $\{\|\text{gp}_{\hat{n}+1}[\hat{\nu}_i]^T AW\|_2\}_{i=1}^{\hat{n}}$
 - 6: **return** ν
-

Algorithm 6.2 Estimating $\sigma(\Lambda)$ using multiple time traces.

- 1: Inputs: Time traces $\{Z_i\}_{i=1}^M$, bounds on DMD order (n_{min}, n_{max}) and number of permitted delays (del_{min}, del_{max}).
 - 2: $\mathcal{I} := 1 : M$, $\mathcal{J} := n_{min} : n_{max}$, $\mathcal{K} := del_{min} : del_{max}$.
 - 3: **for** $i \in \mathcal{I}$ **do**
 - 4: **for** $j \in \mathcal{J}$ **do**
 - 5: **for** $k \in \mathcal{K}$ **do**
 - 6: $(\tilde{c}_{ijk})_{c_{ijk}} :=$ Result of (mean-subtracted) Companion DMD of order j on the k delayed version of the i -th time series.
 - 7: $w_{ijk} :=$ Non-negative weight indicating the reliability of c_{ijk} .
 - 8: $(\delta_{rel}^\mu)_{ijk} := \delta_{rel}^\mu[\tilde{c}_{ijk}]$.
 - 9: **end for**
 - 10: **end for**
 - 11: **end for**
 - 12: Generate a box-whisker plot of $\{(\delta_{rel}^\mu)_{ijk}\}$. This will resemble the plots in [Figure 6.1](#).
 - 13: Pick any integer $n_d^* \geq n_{max} - 1$.
 - 14: Choose \hat{r}_{min} and \hat{r}_{max} such that when $\#[delays] = n_d^*$, the jump in δ_{rel}^μ occurs for $\hat{r}_{min} \leq n \leq \hat{r}_{max}$.
 - 15: **for** $s = \hat{r}_{min} : \hat{r}_{max}$ **do**
 - 16: $\hat{\nu}_s :=$ Output of [Algorithm 6.1](#) with inputs: $\{c_{isk}\}_{i \in \mathcal{I}, k \in \mathcal{K}_{\geq s-1}}, \{w_{isk}\}_{i \in \mathcal{I}, k \in \mathcal{K}_{\geq s-1}}, s$
 - 17: **end for**
 - 18: Choose s^* such that $\rho_{subset}[\hat{\nu}_{s^*}, \hat{\nu}_{s^*+j}] \ll 1$ for $j \geq 1$.
 - 19: **return** $\hat{\nu}_{s^*}$
-

[Algorithm 6.2](#), applied to LTI_1 and LTI_2 , estimated¹³ the respective spectra to within a Hausdorff distance of 10^{-7} . This is reflected in the checks for [Corollary 5.2](#): [Figure 6.5](#) is effectively made of the respective panels in [Figures 6.3](#) and [6.4](#).

¹²Further details of this development can be found in [Appendix F.2](#)

¹³For all computations, we use $n_d^* = n_{max} - 1$

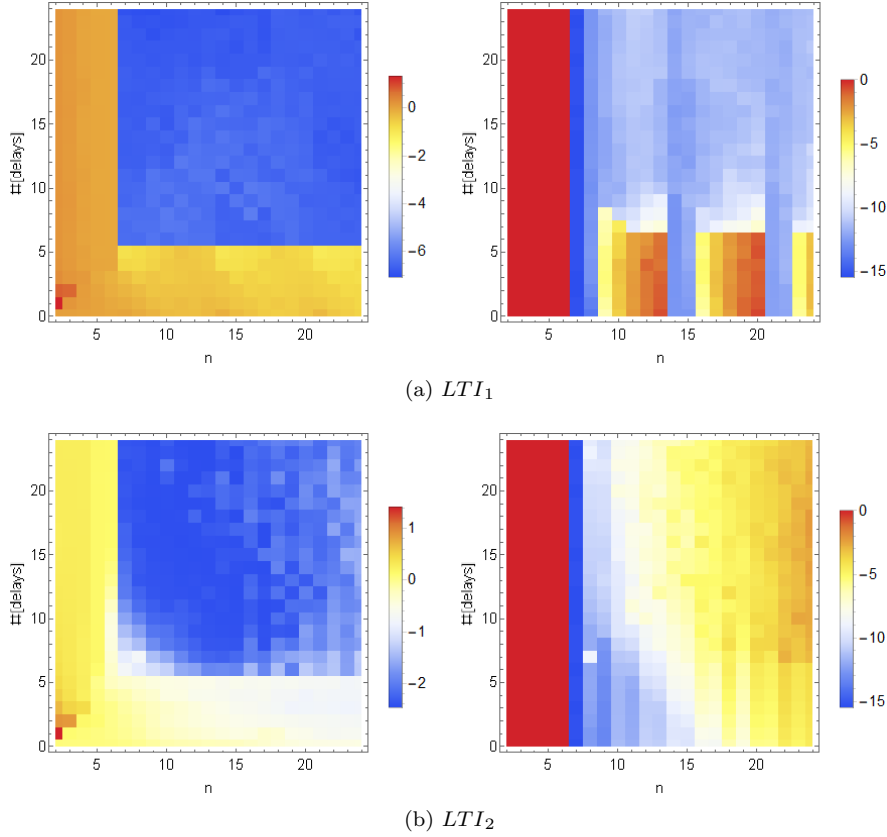
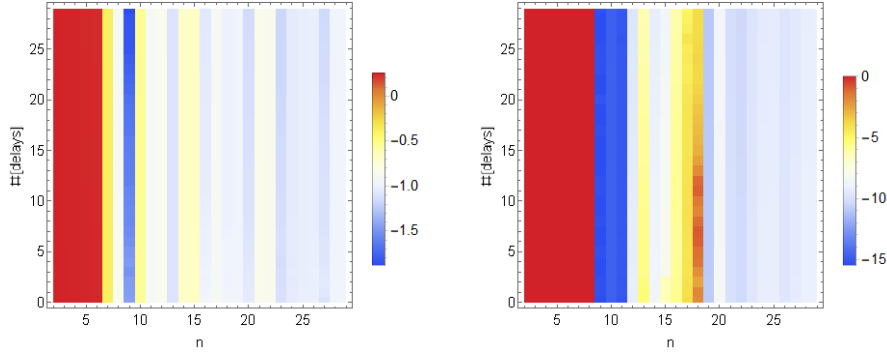


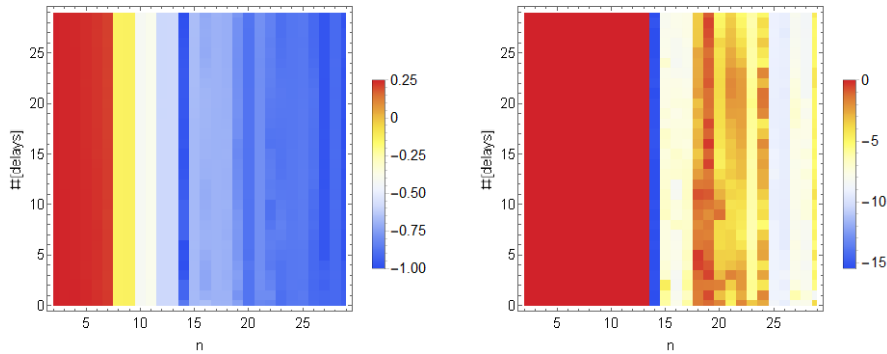
FIG. 6.5. Verifying [Corollary 5.2](#) for LTI_1 and LTI_2 , using the spectral estimate from [Algorithm 6.2](#). Qualitatively, (a) and (b) are the same as (a) in [Figures 6.3](#) and [6.4](#) respectively.

Cavity flow at $Re = 13k, 16k$ and $20k$ is estimated to have $r = 9, 14$ and 25 respectively. This correlates with the growing richness of the underlying dynamics. Although devoid of variations with increasing delays, ρ_{subset} exhibits a unique global minimum for $n = r$. This valley develops a friendlier gradient at larger values of Re , in both the under and over-sampled regimes. During the former, raising n brings a subset of the DMD spectrum closer to the estimated Koopman spectrum, in the Hausdorff sense. In the latter data-rich region, all model orders fare better than their under-sampled contemporaries and contain the estimated spectrum to within one decimal point. Despite this mild uncertainty, the worst case value of $\delta_{trivial}$ here is around 0.05 , while the median rises, alongside Re , from 10^{-5} to 10^{-2} . Hence, the same set of modes effectively accounts for at least 95% the dynamics, even with a high-fidelity model possessing twice the degrees of freedom.

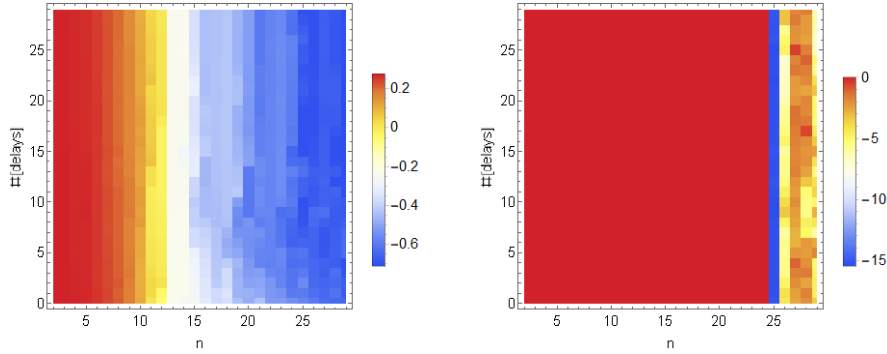
7. Conclusions and Future Work. The relationship between mean subtracted DMD and temporal DFT has been clarified. When the observables are in some finite dimensional Koopman invariant subspace, equivalence signals the need for more data. Non-equivalence indicates data sufficiency, for data that has a minimum number of time delays. However, this number depends on the dimension of the underlying invariant subspace. In other words, equivalence can be used to deduce a lack of data from the mere existence of a finite invariant subspace. In contrast, non-equivalence requires



(a) $Re = 13,000$, $r \approx 9$



(b) $Re = 16,000$, $r \approx 14$



(c) $Re = 20,000$, $r \approx 25$

FIG. 6.6. Verifying *Corollary 5.2* for $Re = 13k, 16k$ and $20k$. Both indicators drop off after $n = r$ and roughly remain so upon a further increase in n .

an upper bound on the dimension of the subspace before any inference. An ironic interlude to this venture: What was viewed a potential rot, now proven transient, is a reliable indicator of sampling requirements.

In the same setting, pruning DMD eigenvalues based on the norm of the corresponding DMD modes has been justified when data is sufficient. This holds regardless of mean-subtraction, although the affirmative requires additional pre-processing before DMD.

Many aspects of this problem are open for study. A pragmatic question would be to investigate the statistics of DMD-DFT equivalence for a better estimate of the transition point. Similarly, a refined approach to leveraging non-equivalence in understanding sampling requirements is lacking. The strategy in this work is to guess an upper bound on the subspace dimension, and increase it whenever a contradicting data-point is seen. This is a potentially Sisyphean task when working purely with data. A more theoretical pursuit would be to relax the assumptions of distinct eigenvalues and a finite invariant subspace. The latter generalization might be of greater import in understanding failure mechanisms of [Algorithm 6.2](#), and its subsequent robustification.

Acknowledgments. This work was supported by the Army Research Office (ARO-MURI W911NF-17-1-030) and the National Science Foundation (Grant no. 1935327).

Appendix A. Notations redux.

A.1. Sets.

$$(\mathbb{C}_\infty)_\infty := \cup_{j=1}^\infty (\mathbb{C}_\infty)^j$$

(All finite tuples of finite dimensional vectors)

$$l_2^D := \{\alpha \in \mathbb{C}^\mathbb{N} \mid \exists N(\alpha) \text{ such that } \forall n \geq N(\alpha), \alpha_n = 0\}$$

(All sequences with finite non-zero terms)

$$P := \{f \mid \forall z \in \mathbb{C}, f(z) = \sum_{i=0}^\infty \alpha_{i+1} z^i, \alpha \in l_2^D\}$$

(All polynomials)

$$P_n := \{f \mid \forall z \in \mathbb{C}, f(z) = \sum_{i=0}^n \alpha_{i+1} z^i, \alpha \in \mathbb{C}^{n+1}\}$$

(All polynomials of degree at most n)

A.2. Matrix-vector operations.

- Additional index notation for matrices:

$$A_{1:-2} := [a_j]_{j=1}^{n-1} = [a_{ij}]_{i=1, j=1}^{m, n-1} = \begin{bmatrix} | & | & \cdots & | \\ a_1 & a_2 & \cdots & a_{n-1} \\ | & | & & | \end{bmatrix}$$

$$A_{2:-1} := [a_j]_{j=2}^n = [a_{ij}]_{i=1, j=2}^{m, n} = \begin{bmatrix} | & | & \cdots & | \\ a_2 & a_3 & \cdots & a_n \\ | & | & & | \end{bmatrix}$$

- The outer product of two vectors, a and b , is written as $a \otimes b = ab^H$.

Appendix B. On DMD-DFT equivalence.

B.1. Some logistical observations.

B.1.1. Vandermonde ventures.

- Observables in a Koopman invariant subspace have a parsimonious expression

for the relevant Z :

$$\begin{aligned}
\forall j \in \mathbb{Z}, z_{j+1} &:= \Psi(x_{j+1}) \\
&= \Psi(\top^j(x_1)) \\
&= \tilde{C}\Phi(\top^j(x_1)) \\
&= \tilde{C}U^j\Phi(x_1) \\
&= \tilde{C}\Lambda^j\Phi(x_1) \\
&= C[\lambda_i^j]_{i=1}^r \\
\implies Z &= C\Theta
\end{aligned}$$

- Θ and its subsets are pervasive:

$$\begin{aligned}
\mu &= C\Theta \frac{\mathbf{1}_{n+1}}{n+1} \\
X_{ms} &= C \left(\Theta_1 - \Theta \frac{\mathbf{1}_{n+1}}{n+1} \mathbf{1}_n^T \right)
\end{aligned}$$

- Notational utility of gp_{n+1} in denoting Θ :

$$\begin{aligned}
\overline{\text{gp}_{n+1}[\bar{\lambda}]} &= \text{gp}_{n+1}[\bar{\lambda}] \\
\Theta &= \sum_{j=1}^r e_j \text{gp}_{n+1}[\lambda_j]^T \\
&= \sum_{j=1}^r e_j \otimes \text{gp}_{n+1}[\bar{\lambda}_j] \\
\text{msub}_{n+1}[1] &= \mathcal{P}_{\mathcal{N}(\mathbf{1}_{n+1}^H)}
\end{aligned}$$

B.1.2. Mean subtraction and matrix multiplication. We show that removing the temporal mean of Z with respect to λ can be re-written as post-multiplication of Z by the matrix $\text{msub}_{n+1}[\lambda]$. When $Z = \Theta$ and $\lambda \neq 0$, mean subtraction is also equivalent to pre-multiplying an augmented Vandermonde matrix $\tilde{\Theta}$ by $\text{pre}_{n+1}[\lambda]$.

Subtracting the temporal mean of Z is tantamount to a matrix multiplication. To see this, we begin with the following definition:

$$\begin{aligned}
\text{msub}_{n+1} &: \mathbb{C} \rightarrow \mathbb{C}^{(n+1) \times (n+1)} \\
\text{msub}_{n+1}[\lambda] &:= I_{n+1} - \left(\frac{1}{n+1} \right) \text{gp}_{n+1}[\lambda^{-1}] \text{gp}_{n+1}[\lambda]^T
\end{aligned}$$

Evaluating msub_{n+1} at λ , we observe:

$$\begin{aligned}
Z \text{msub}_{n+1}[\lambda] &= Z - \left(\frac{1}{n+1} \right) Z \text{gp}_{n+1}[\lambda^{-1}] \text{gp}_{n+1}[\lambda]^T \\
&= Z - \mu_\lambda \text{gp}_{n+1}[\lambda]^T
\end{aligned} \tag{5.1}$$

$$\begin{aligned}
\implies (Z \text{msub}_{n+1}[\lambda])_i &= z_i - \mu_\lambda \lambda^{i-1} \\
&= (Z_{ms}^\lambda)_i
\end{aligned} \tag{5.2}$$

To see that $Z = \Theta$ allows us to flip the effect of mean subtraction, some tedious

book-keeping of momentary import is required:

$$\begin{aligned}
\zeta &: \mathbb{C} \rightarrow \mathbb{C}^r \\
\zeta_\lambda &:= \Theta \frac{\text{gp}_{n+1}[\lambda^{-1}]}{n+1} \\
\text{pre}_{n+1} &: \mathbb{C} \rightarrow \mathbb{C}_{\infty \times \infty} \\
\text{pre}_{n+1}[\lambda] &:= \begin{cases} \begin{bmatrix} I - \zeta_\lambda e_i^T \\ I - \zeta_\lambda \end{bmatrix} & \lambda = \lambda_i \\ \begin{bmatrix} I & -\zeta_\lambda \end{bmatrix} & \lambda \notin \sigma(A) \end{cases} \\
\tilde{\Theta}, \tilde{\Theta}_1 &: \mathbb{C} \rightarrow \mathbb{C}_{\infty \times \infty} \\
\tilde{\Theta}[\lambda] &:= \begin{cases} \Theta & \lambda = \lambda_i \\ \begin{bmatrix} \Theta \\ \text{gp}_{n+1}[\lambda]^T \end{bmatrix} & \lambda \notin \sigma(A) \end{cases} \\
\tilde{\Theta}_1[\lambda] &:= (\tilde{\Theta}[\lambda])_{1:-2}
\end{aligned}$$

We now show that pre-multiplying $\tilde{\Theta}$ with $\text{pre}_{n+1}[\lambda]$ produces the same effect as removing the mean of Θ with respect to λ .

LEMMA B.1.

$$\forall \lambda \neq 0, \Theta \text{msub}_{n+1}[\lambda] = \text{pre}_{n+1}[\lambda] \tilde{\Theta}$$

Proof.

$$\begin{aligned}
\Theta \text{msub}_{n+1}[\lambda] &= \Theta \left(I_{n+1} - \left(\frac{1}{n+1} \right) \text{gp}_{n+1}[\lambda^{-1}] \text{gp}_{n+1}[\lambda]^T \right) \\
&= \Theta - \left(\frac{1}{n+1} \right) \Theta \text{gp}_{n+1}[\lambda^{-1}] \text{gp}_{n+1}[\lambda]^T \\
&= \Theta - \zeta_\lambda \text{gp}_{n+1}[\lambda]^T \\
&= \left(\sum_{j=1}^r e_j \text{gp}_{n+1}[\lambda_j]^T \right) - (\zeta_\lambda \text{gp}_{n+1}[\lambda]^T) \\
&= \begin{cases} [I - \zeta_\lambda e_i^T] \Theta & \lambda = \lambda_i \\ \begin{bmatrix} I & -\zeta_\lambda \\ & \text{gp}_{n+1}[\lambda]^T \end{bmatrix} \Theta & \lambda \notin \sigma(A) \end{cases} \\
&= \text{pre}_{n+1}[\lambda] \tilde{\Theta}
\end{aligned}$$

□

B.2. Proofs of main results.

Proof of Theorem 4.1. We begin with the backward implication.

$$\begin{aligned}
c_{ms} &= X_{ms}^\dagger (z_{n+1} - \mu) \\
\implies c_{ms} &\in \mathcal{R}(X_{ms}^H) \\
\implies c_{ms} &\perp \mathcal{N}(X_{ms}) \\
\implies \mathcal{P}_{\mathcal{N}(X_{ms})} c_{ms} &= 0 \\
\implies \mathcal{P}_{\mathcal{N}(X_{ms})} \mathbf{1}_n &= 0
\end{aligned}$$

The forward implication proceeds by observing that $X_{ms}(-\mathbf{1}_n) = y_{ms}$ [7]. Indeed, $c = -\mathbf{1}_n + d$ has zero residue for any $d \in \mathcal{N}(X_{ms})$. However, c_{ms} is the *minimum norm* solution. To this end, we use the fact that $I = \mathcal{P}_{\mathcal{N}(X_{ms})} + \mathcal{P}_{R(X_{ms}^H)}$ and make the following observations:

$$\begin{aligned} \mathbf{1}_n &= \mathcal{P}_{R(X_{ms}^H)}\mathbf{1}_n, & (\mathcal{P}_{\mathcal{N}(X_{ms})}\mathbf{1}_n &= 0) \\ d &= \mathcal{P}_{\mathcal{N}(X_{ms})}d, & (d \in \mathcal{N}(X_{ms})) \\ \implies \mathcal{P}_{R(X_{ms}^H)}c &= -\mathbf{1}_n, & \mathcal{P}_{\mathcal{N}(X_{ms})}c &= d \end{aligned}$$

Using the same technique on c , we see:

$$\begin{aligned} c &= \mathcal{P}_{\mathcal{N}(X_{ms})}c + \mathcal{P}_{R(X_{ms}^H)}c \\ \implies \|c\|^2 &= \|d\|^2 + \|\mathbf{1}_n\|^2 \end{aligned}$$

Therefore, the minimum norm solution corresponds to $d = 0$. Hence, $c_{ms} = -\mathbf{1}_n$. \square

A Vandermonde matrix has linearly independent rows iff it has at least as many columns as rows and its nodes are distinct.

LEMMA B.2. [13]

$$\forall i, j, \lambda_i \neq \lambda_j \ \& \ n \geq r \iff \Theta_1 \text{ has full row rank.}$$

All dependencies required to show that oversampling prevents DMD-DFT equivalence are now in place.

Proof of Theorem 4.2. We note the following expression for X_{ms} :

$$\begin{aligned} X_{ms} &= (Z_{ms}^1)_{1:-2} \\ &= (Z_{msub_{n+1}}[1])_{1:-2} \\ &= (C\Theta_{msub_{n+1}}[1])_{1:-2} \\ &= (Cpre_{n+1}[1]\tilde{\Theta})_{1:-2} \\ &= Cpre_{n+1}[1](\tilde{\Theta})_{1:-2} \\ &=: Cpre_{n+1}[1]\tilde{\Theta}_1 \end{aligned}$$

Suppose $\mathbf{1}_n \in \mathcal{R}(X_{ms}^H) \iff \exists \tilde{d}$ such that $\tilde{d}^H X_{ms} = \mathbf{1}_n^H$

$$\begin{aligned} \tilde{d}^H X_{ms} &= \mathbf{1}_n^H \\ \tilde{d}^H Cpre_{n+1}[1]\tilde{\Theta}_1 &= \mathbf{1}_n^H \\ d^H pre_{n+1}[1]\tilde{\Theta}_1 &:= \mathbf{1}_n^H \\ \implies d^H pre_{n+1}[1]\tilde{\Theta}_1 - \mathbf{1}_n^H &= \begin{cases} \begin{bmatrix} d^H & -d^H\zeta_1 - 1 \end{bmatrix} \begin{bmatrix} \Theta_1 \\ \mathbf{1}_n^H \end{bmatrix} & 1 \notin \sigma(A) \\ \begin{bmatrix} d^H [I - \zeta_1 e_i^H] - e_i^H \end{bmatrix} \Theta_1 & \lambda_i = 1 \end{cases} \\ &= 0 \end{aligned}$$

$\lambda_i = 1 \implies d^H(I - \zeta_1 e_i^H) - e_i^H \neq 0$. This can be proved by contradiction. For if this was false, we would have:

$$\begin{aligned} d^H(I - \zeta_1 e_i^H) &= e_i^H \\ d^H &= (1 + d^H\zeta_1)e_i^H \\ d^H\zeta_1 &= (1 + d^H\zeta_1) \quad (e_i^H\zeta_1 = 1) \\ 0 &= 1 \end{aligned}$$

which is a contradiction. Hence, we have a $(r \times n)$ or $(r + 1) \times n$ Vandermonde matrix with linearly dependent rows. By [Lemma B.2](#), $n < r$ or $n < r + 1$ which is a contradiction. Hence,

$$\begin{aligned} & \mathbf{1}_n \notin \mathcal{R}(X_{ms}^H) \\ \implies & \mathcal{P}_{\mathcal{N}(X_{ms})} \mathbf{1}_n \neq 0 \\ \implies & c_{ms} \neq -\mathbf{1}_n \quad (\text{Theorem 4.1}) \quad \square \end{aligned}$$

Proving [Corollary 4.3](#) is tedious, for the wrong reasons. The pragmatic case of under-sampling is a direct application [Theorem 3.3](#). In contrast, the just-sampled regime, which potentially constitutes a small fraction of the set of hyper-parameters tested, requires a disproportionate amount of algebra.

Proof of Corollary 4.3. The general idea here is to prove or disprove the existence of elements of $\mathcal{N}(X_{ms})$ that have specific properties.

$$\begin{aligned} \forall c, \quad X_{ms}c &= C \left(\Theta_1 - \Theta \frac{\mathbf{1}_{n+1}}{n+1} \mathbf{1}_n^H \right) c \\ &= C \Theta \begin{bmatrix} c - \mathbf{1}_n \left(\frac{\mathbf{1}_n^H c}{n+1} \right) \\ -\frac{\mathbf{1}_n^H c}{n+1} \end{bmatrix} \\ &= C \Theta \begin{bmatrix} c - \mathbf{1}_n v[c] \\ -v[c] \end{bmatrix} \quad \left(v[c] := \frac{\mathbf{1}_n^H c}{n+1} \right) \end{aligned}$$

For the sake of brevity, we drop the dependence on c unless relevant.

$$\begin{aligned} \text{Assume } \exists c \neq 0 \in \mathcal{N}(X_{ms}) \\ \implies & X_{ms}c = 0 \\ \implies & C \Theta \begin{bmatrix} \mathbf{1}_n v - c \\ v \end{bmatrix} = 0 \\ \implies & \Theta \begin{bmatrix} \mathbf{1}_n v - c \\ v \end{bmatrix} = 0 \quad (\tilde{C} \text{ is full column rank}) \end{aligned}$$

$n = r$: Θ_1 is invertible and hence, $v \neq 0$. In addition, $\mathcal{N}(\Theta) = \mathcal{R} \left(\begin{bmatrix} c_p \\ 1 \end{bmatrix} \right)$, where the entries of $\tilde{c} := \begin{bmatrix} c_p \\ 1 \end{bmatrix}$ are the coefficients of the unique degree r monic polynomial whose roots are $\sigma_1(A)$. Hence, we have

$$\begin{aligned} & v \neq 0 \\ & \begin{bmatrix} \mathbf{1}_n v - c \\ v \end{bmatrix} = v \begin{bmatrix} c_p \\ 1 \end{bmatrix} \\ \implies & v + nv - \mathbf{1}_n^H c = v(\mathbf{1}_n^H c_p + 1) \\ \implies & \mathbf{1}_{n+1}^H \tilde{c} = 0 \end{aligned}$$

\Leftarrow :

$$\begin{aligned} & 1 \notin \sigma_1(A) \\ \implies & \mathbf{1}_{n+1}^H \tilde{c} \neq 0 \quad (\text{Fundamental Theorem of Algebra}) \end{aligned}$$

This is a contradiction. Hence, $\mathcal{N}(X_{ms}) = \phi \implies c_{ms} = -\mathbf{1}_n$. Using [Theorem 3.1](#) and a guess of \mathcal{F} , we can see that mean-subtracted DMD is DFT.

\implies (Via contraposition)

Here, we construct a vector in $\mathcal{N}(X_{ms})$ that has a non-zero inner product with $\mathbf{1}_n$.

$$\begin{aligned}
& 1 \in \sigma(A) \\
& \implies \mathbf{1}_{n+1}^H \tilde{c} = 0 \\
& \quad \mathbf{1}_n^H c_p = -1 \\
& \implies c_p \neq \mathbf{1}_n \\
& c := \mathbf{1}_n - c_p \\
& \implies c \neq 0 \\
& v[c] = \frac{\mathbf{1}_n^H c}{n+1} \\
& \quad = \frac{n - \mathbf{1}_n^H c_p}{n+1} \\
& \quad = 1 \\
& \implies X_{ms}c = -C\Theta \begin{bmatrix} \mathbf{1}_n - c \\ 1 \end{bmatrix} \\
& \quad = -C\Theta \begin{bmatrix} c_p \\ 1 \end{bmatrix} \\
& \quad = -C\Theta \tilde{c} \\
& \quad = 0 \\
& \implies c \in \mathcal{N}(X_{ms}) \\
& \mathbf{1}_n^H c \neq 0 \implies c_{ms} \neq -\mathbf{1}_n \quad (\text{Theorem 4.1})
\end{aligned}$$

The final case of $n < r$ falls readily from [Theorem 3.3](#).

$$n < r \implies \mathcal{N}(\Theta) = \phi$$

$$\implies Z = C\Theta \text{ has full column rank} \quad (\tilde{C} \text{ has full column rank})$$

By [Theorem 3.3](#), mean subtracted DMD is equivalent to temporal DFT. \square

Appendix C. Polynomials and matrix algebra. The overarching idea explored in this section is that certain matrix-vector operations are equivalent to manipulating uni-variate polynomials [8, 30]. An endemic benefit of adopting this perspective is seen in [Corollary 4.3](#), where interpreting a vector (\tilde{c}) as the coefficients of a polynomial proved quite fruitful.

C.1. Basic operations. We define some common operations on polynomials. We use two polynomials, $f_1[x] := x^2 - 2x + 1$ and $f_2[x] := -3x + 3x^3$ as examples. [Figure C.1](#) summarizes this section in the context of f_2 .

poly maps any finite dimensional vector to a polynomial.

$$\begin{aligned}
& \text{poly} : \mathbb{C}_\infty \rightarrow P \\
& \forall \alpha \in \mathbb{C}_\infty, \\
& \text{poly}_\alpha : \mathbb{C} \rightarrow \mathbb{C} \\
& \text{poly}_\alpha[z] := \sum_{i=0}^{\#\alpha-1} \alpha_{i+1} z^i
\end{aligned}$$

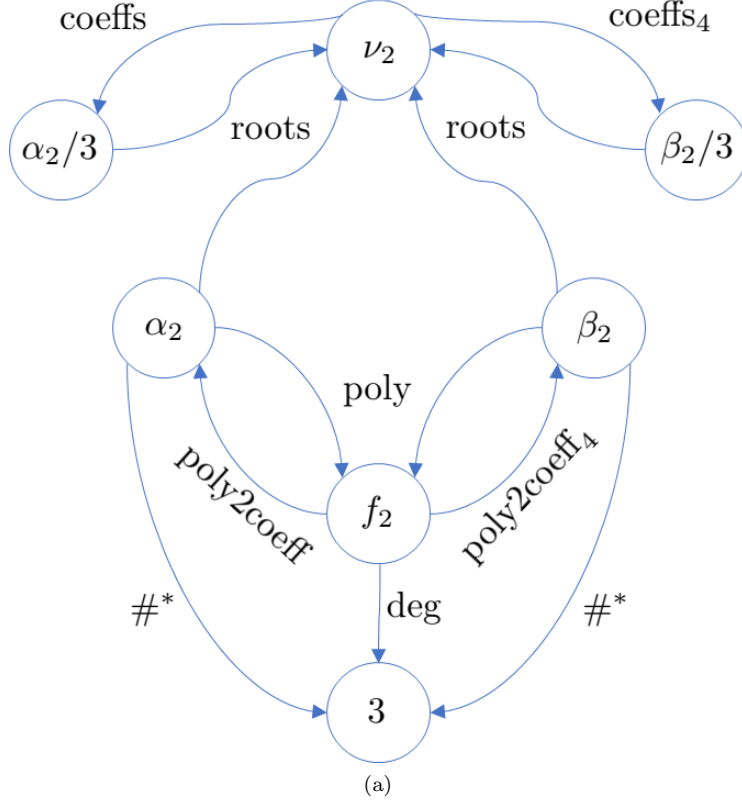


FIG. C.1. An illustration of polynomial manipulations using $f_2[x] := -3x + 3x^3$. Here, $\alpha_2 = [0 \ -3 \ 0 \ 3]^H$, $\beta_2 = [0 \ -3 \ 0 \ 3 \ 0]^H$ and $\nu_2 = [1 \ -1 \ 0]^H$.

Specifically, we have:

$$\begin{aligned} \alpha_1 &:= [1 \ -2 \ 1]^H \implies f_1[z] = \text{poly}_{\alpha_1}[z] \\ \alpha_2 &:= [0 \ -3 \ 0 \ 3]^H \implies f_2[z] = \text{poly}_{\alpha_2}[z] \end{aligned}$$

This mapping is not injective. For instance,

$$\begin{aligned} \beta_1 &:= [1 \ -2 \ 1 \ 0 \ 0]^H \implies \text{poly}_{\beta_1}[z] = f_1[z] = \text{poly}_{\alpha_1}[z] \\ \beta_2 &:= [0 \ -3 \ 0 \ 3 \ 0]^H \implies \text{poly}_{\beta_2}[z] = f_2[z] = \text{poly}_{\alpha_2}[z] \end{aligned}$$

Observe that the standard basis vectors are mapped to monomials.

$$\begin{aligned} \forall i \in \mathbb{N}, \text{poly}_{e_i}[z] &= z^{i-1} \\ \implies \text{poly}_{\alpha} &= \sum_{i=1}^{\#\alpha} \alpha_i \text{poly}_{e_i} \end{aligned}$$

Furthermore, the action of the Vandermonde matrix Θ on a vector x can be seen as sampling a polynomial at $\{\lambda_i\}_{i=1}^r$

$$\Theta x = [\text{poly}_x[\lambda_i]]_{i=1}^r = [\text{poly}_x[\lambda_1] \ \text{poly}_x[\lambda_2] \ \dots \ \text{poly}_x[\lambda_r]]^T$$

deg finds the degree of a polynomial, and $\#^*$ is the equivalent definition for vectors¹⁴.

$$\begin{aligned}\text{deg} &: P \rightarrow \mathbb{W} \\ \text{deg}[f] &:= (\max\{i \mid \alpha_i \neq 0\}) - 1 \\ \#^* &: \mathbb{C}_\infty \rightarrow \mathbb{N} \\ \#^*[\alpha] &:= \text{deg}[\text{poly}_\alpha]\end{aligned}$$

For f_1, f_2 , we have:

$$\begin{aligned}\text{deg}[f_1] &= \#^*[\alpha_1] = \#^*[\beta_1] = 2 \\ \text{deg}[f_2] &= \#^*[\alpha_2] = \#^*[\beta_2] = 3\end{aligned}$$

poly2coeff_n and poly2coeff map a polynomial to its coefficient vector. The latter gives the most concise vector, while the former appends zeros to give a $(n + 1)$ -D vector

$$\begin{aligned}\text{poly2coeff}_n &: P_n \rightarrow \mathbb{C}^{n+1} \\ \text{poly2coeff} &: P \rightarrow \mathbb{C}_\infty \\ f &= \sum_{i=0}^n \alpha_{i+1} \text{poly}_{e_{i+1}} \\ \implies \text{poly2coeff}_n[f] &:= [\alpha_{i+1}]_{i=0}^n \\ \text{poly2coeff}[f] &:= \text{poly2coeff}_{\text{deg}[f]}[f]\end{aligned}$$

This gives:

$$\begin{aligned}\text{poly2coeff}_4[f_1] &= \beta_1 & \text{poly2coeff}_4[f_2] &= \beta_2 \\ \text{poly2coeff}[f_1] &= \alpha_1 & \text{poly2coeff}[f_2] &= \alpha_2\end{aligned}$$

More generally, we see:

$$\begin{aligned}\forall \alpha \in \mathbb{C}_\infty, f \in P \ \& \ \omega \in \mathbb{C}, \\ \text{poly2coeff} \circ \text{poly}_\alpha &= \alpha \\ \text{poly}_{\text{poly2coeff}[f]} &= f \\ \text{poly2coeff}[\omega f] &= \omega \text{poly2coeff}[f]\end{aligned}$$

roots gives the roots of the polynomial represented by the argument.

$$\begin{aligned}\text{roots} &: \mathbb{C}_\infty \rightarrow \mathbb{C}_\infty \\ \text{roots}[\alpha] &:= [\nu_j]_{j=1}^{\#^*[\alpha]} \text{ simultaneously satisfying} \\ &\begin{cases} \forall j, \sum_{i=0}^{\#^*[\alpha]-1} \alpha_{i+1} (\nu_j)^i = 0 \\ \forall j \leq k, |\nu_j| \geq |\nu_k| \end{cases}\end{aligned}$$

This gives:

$$\begin{aligned}\nu_1 &:= \text{roots}[\alpha_1] = \begin{bmatrix} 1 & 1 \end{bmatrix}^H = \text{roots}[\beta_1] \\ \nu_2 &:= \text{roots}[\alpha_2] = \begin{bmatrix} 1 & -1 & 0 \end{bmatrix}^H = \text{roots}[\beta_2]\end{aligned}$$

¹⁴Technically, $\#^*$ is the pull-back of deg via poly onto \mathbb{C}_∞

coeffs gives the coefficients of the unique monic polynomial whose roots comprise the input. coeffs_n is analogous to poly2coeff_n, as it appends 0s to the output of coeffs to create a (n + 1)D vector

$$\begin{aligned}
& \text{coeffs} : \mathbb{C}_\infty \cup \{\emptyset\} \rightarrow \mathbb{C}_\infty \\
& \text{coeffs}[\nu] := [a_j]_{j=1}^{\#\nu+1} \text{ simultaneously satisfying} \\
& \quad \begin{cases} \forall j, \sum_{i=0}^{\#\nu} a_{i+1}(\nu_j)^i = 0 \\ a_{\#\nu+1} = 1 \end{cases} \\
& \text{coeffs}_n : \mathbb{C}_\infty \cup \{\emptyset\} \rightarrow \mathbb{C}^n \\
& \forall \nu \text{ such that } n \geq \#\nu, \\
& \text{coeffs}_n[\nu] := \text{poly2coeff}_n[\text{poly_coeffs}[\nu]] \\
& \quad = \begin{bmatrix} \text{coeffs}[\nu] \\ \mathbf{0}_{n-\#\nu} \end{bmatrix}
\end{aligned}$$

For the examples under study, we get:

$$\begin{aligned}
\text{coeffs}[\nu_1] &= [1 \quad -2 \quad 1]^H \\
&= \alpha_1 \\
\text{coeffs}_4[\nu_1] &= \beta_1 \\
\text{coeffs}[\nu_2] &= [0 \quad -1 \quad 0 \quad 1]^H \\
&= \alpha_2/3 \\
\text{coeffs}_4[\nu_2] &= \beta_2/3
\end{aligned}$$

- Roots are unchanged by a non-zero scaling : $\forall t \in \mathbb{C} - \{0\}, \text{roots}[t\alpha] = \text{roots}[\alpha]$.
- coeffs followed by roots is effectively a permutation : $\text{roots} \circ \text{coeffs} \stackrel{\Pi}{=} I$
- The reverse is equivalent to a non-zero scaling by t : $\text{coeffs} \circ \text{roots} \stackrel{t}{=} I$

C.2. Polynomial addition. Adding 2 polynomials amounts to summing their appropriate coefficient vectors. For instance,

$$\begin{aligned}
f_1[x] + f_2[x] &= (1 - 2x + 1x^2 + 0x^3) \\
&\quad + (0 - 3x + 0x^2 + 3x^3) \\
&= 1 - 5x + x^2 + 3x^3 \\
\implies \text{poly2coeff}[f_1 + f_2] &= [1 \quad -5 \quad 1 \quad 3]^H \\
&= \text{poly2coeff}_3[f_1] + \text{poly2coeff}_3[f_2]
\end{aligned}$$

Extrapolating, we get:

$$\begin{aligned}
(C.1) \quad & g := \sum_{i=1}^n \text{poly}_{x_i} \\
& \theta := \text{deg}[g] \\
\implies \text{poly2coeff}(g) &= \text{poly2coeff}_\theta \left[\sum_{i=1}^n \text{poly}_{x_i} \right] \\
&= \sum_{i=1}^n \text{poly2coeff}_\theta[\text{poly}_{x_i}]
\end{aligned}$$

C.3. Polynomial multiplication. Multiplying two polynomials is equivalent to a matrix vector product in coefficient space. This can be seen by multiplying f_1 & f_2 .

$$\begin{aligned}
(f_1 f_2)[x] &= (1 - 2x + x^2)(-3x + 3x^3) \\
&= (1 - 2x + x^2)(-3x) + (1 - 2x + x^2)(3x^3) \\
&= (-3x + 3x^3)(1) + (-3x + 3x^3)(-2x) + (-3x + 3x^3)(x^2) \\
\Rightarrow \text{poly2coeff}[f_1 f_2] &= \begin{bmatrix} 1 & & & & \\ -2 & 1 & & & \\ 1 & -2 & 1 & & \\ & 1 & -2 & 1 & \\ & & 1 & -2 & 1 \\ & & & 1 & \end{bmatrix} \begin{bmatrix} 0 \\ -3 \\ 0 \\ 3 \end{bmatrix} \\
&= \begin{bmatrix} -3 & & & & \\ & -3 & & & \\ 3 & & -3 & & \\ & & 3 & & \\ & & & 3 & \end{bmatrix} \begin{bmatrix} 1 \\ -2 \\ 1 \end{bmatrix}
\end{aligned}$$

This motivates the following definition:

$$\begin{aligned}
&\text{band} : \mathbb{C}_\infty \times \mathbb{N} \rightarrow \mathbb{C}_{\infty \times \infty} \\
\text{(C.2)} \quad \text{band}[\alpha, r] &:= [\text{poly2coeff}_\theta[\text{poly}_\alpha \text{poly}_{e_j}]]_{j=1}^r \\
&\theta := \#\alpha + r - 2
\end{aligned}$$

Consequently, $f_1 f_2$ can be expressed compactly:

$$\text{poly2coeff}[f_1 f_2] = \text{band}[\alpha_1, 4]\alpha_2 = \text{band}[\alpha_2, 3]\alpha_1$$

Hence, band creates a banded matrix by successive forward shifts of a coefficient vector. Another interpretation is that the columns of $\text{band}[\alpha, r]$ represent polynomials with additional roots at 0. This obtains from the fact that a product of polynomials has all the roots of its arguments¹⁵, i.e

$$\begin{aligned}
\text{poly}_\beta &= \text{poly}_{\alpha_1} \text{poly}_{\alpha_2} \\
\Rightarrow \text{roots}[\beta] &\stackrel{\Pi}{=} \begin{bmatrix} \text{roots}[\alpha_1] \\ \text{roots}[\alpha_2] \end{bmatrix}
\end{aligned}$$

The following lemma formalizes this interpretation of polynomial products.

LEMMA C.1.

$$\begin{aligned}
&\alpha \in \mathbb{C}^{n+1}, \beta \in \mathbb{C}^{m+1} \\
&\alpha_{n+1}, \beta_{m+1} \neq 0 \\
&\text{poly2coeff}(\text{poly}_\alpha \text{poly}_\beta) = \text{band}[\alpha, m+1]\beta = \text{band}[\beta, n+1]\alpha
\end{aligned}$$

¹⁵ $x \stackrel{\Pi}{=} y$ denotes component-wise equality of x & y up to a permutation.

Proof.

$$\begin{aligned}
& \alpha_{n+1}, \beta_{m+1} \neq 0 \\
\implies & \#^*[\alpha] = n \ \& \ \#^*[\beta] = m \\
& \text{poly}_\beta =: \sum_{j=1}^{m+1} \beta_j \text{poly}_{e_j} \\
& \text{poly}_\alpha \text{poly}_\beta = \sum_{j=1}^{m+1} \beta_j (\text{poly}_{e_j} \text{poly}_\alpha)
\end{aligned}$$

$\text{poly}_\alpha \text{poly}_\beta$ is of degree $\theta := n + m$. Hence,

$$\text{poly2coeff}(\text{poly}_\alpha \text{poly}_\beta) = \sum_{j=1}^{m+1} \text{poly2coeff}_\theta[\beta_j \text{poly}_{e_j} \text{poly}_\alpha] \quad (\text{C.1})$$

$$\begin{aligned}
& = \sum_{j=1}^{m+1} \text{poly2coeff}_\theta[\text{poly}_{e_j} \text{poly}_\alpha] \beta_j \\
& = \text{band}(\alpha, m + 1) \beta \quad (\text{C.2})
\end{aligned}$$

The case with α, β flipped follows by a similar argument. \square

We can now check if a polynomial f , can factor another polynomial g , with a linear algebraic test.

LEMMA C.2.

$$\begin{aligned}
& \alpha \in \mathbb{C}^{n+1}, \beta \in \mathbb{C}^{m+1} \\
& \alpha_{n+1}, \beta_{m+1} \neq 0 \\
f = \text{poly}_\alpha \text{poly}_\beta & \iff \text{poly2coeff}[f] = \text{band}[\alpha, m + 1] \beta = \text{band}[\beta, n + 1] \alpha
\end{aligned}$$

Proof. \implies is a direct consequence of [Lemma C.1](#).

\longleftarrow

$$\begin{aligned}
f & = \text{poly}_{\text{poly2coeff}(f)} \\
& = \text{poly}_{\text{band}(\alpha, m+1)\beta} \\
& = \text{poly}_{\text{poly2coeff}(\text{poly}_\alpha \text{poly}_\beta)} \quad (\text{Lemma C.1}) \\
& = \text{poly}_\alpha \text{poly}_\beta \quad \square
\end{aligned}$$

The reverse implication in [Lemma C.2](#) has been used to find the GCD of 2 polynomials with an uncertainty in their coefficients [8], by a least squares fit.

Appendix D. Authenticating DMD eigenvalues with DMD mode norm.

The objective of this section is to show that when a Koopman invariant subspace (3.16) is over-sampled, a DMD mode is non-trivial iff it corresponds to a Koopman eigenvalue. In other words, spurious DMD eigenvalues will have trivial DMD modes.

To begin with, we show that the null-space of the Vandermonde matrix, Θ , is the column-space of a specific band matrix.

THEOREM D.1. *Let*

$$\begin{aligned}\alpha^* &:= \text{coeffs}[[\lambda_i]_{i=1}^r] \\ A^* &:= \text{band}[\alpha^*, n-r+1] \\ n &\geq r\end{aligned}$$

Then, the following hold:

- A^* is full column rank
- $\mathcal{N}(\Theta) = \mathcal{R}(A^*)$

Proof. Banded structure of A^* guarantees full column rank.

$$\begin{aligned}x &\in \mathcal{N}(\Theta) \\ \iff \Theta x &= 0 \\ \iff \text{poly}_x(\lambda) &= 0, \forall \lambda \in \{\lambda_j\}_{j=1}^r\end{aligned}$$

where Λ By the Fundamental Theorem of Algebra, $\exists \text{poly}_\beta \in P_{n-r} \equiv \beta \in \mathbb{C}^{n-r+1}$ such that:

$$\begin{aligned}\text{poly}_x &= \text{poly}_{\alpha^*} \text{poly}_\beta \\ \iff \text{poly}_2 \text{coeff}(\text{poly}_x) &= \text{band}(\alpha^*, n-r+1)\beta \quad (\text{Lemma C.2}) \\ \iff x &= A^* \beta \quad (\text{C.2}) \\ \iff x &\in \mathcal{R}(A^*) \quad \square\end{aligned}$$

The following lemma provides necessary and sufficient conditions for the non-zero product of Θ and an eigenvector of a specific Companion matrix. This proves handy in ruling out spurious DMD modes in the sequel.

LEMMA D.2. *Let $c \in \mathbb{C}^{n+1}$ and $(\lambda, \bar{w}_\lambda)$ denote a left eigen-pair of $T[c] \iff w_\lambda^H T[c] = \lambda w_\lambda^H$. Further, let v_λ be the corresponding dual vector $\implies w_\lambda^H v_\lambda = 1$. Now, consider an arbitrary $\Xi_{s \times r}$ and suppose the following is true:*

- $\sigma(\Lambda) \subset \sigma(T[c])$.
- Every column of Ξ is non-zero .

Then, we have :

$$\Xi \Theta v_\lambda \neq 0 \iff \lambda \in \sigma(\Lambda)$$

Proof.

$$\begin{aligned}w_\lambda^H &:= [w_1 \quad w_2 \quad \cdots \quad w_n] \\ w_\lambda^H T[c] &= \lambda w_\lambda^H \\ [w_2 \quad w_3 \quad \cdots \quad w_n \quad w_\lambda^H c] &= \lambda [w_1 \quad w_2 \quad \cdots \quad w_n] \\ \therefore w_\lambda^H &= [1 \quad \lambda \quad \cdots \quad \lambda^{n-1}] \quad (\text{Upto a scaling})\end{aligned}$$

The first condition implies that the rows of Θ are left eigenvectors of $T[c]$. In particular,

$$\begin{aligned}\Theta &= \sum_{i=1}^r e_i \otimes w_{\lambda_i} \\ \Xi \Theta v_\lambda &= \Xi \left(\sum_{i=1}^r e_i (w_{\lambda_i}^H v_\lambda) \right) \\ &= \begin{cases} \Xi e_j & \lambda = \lambda_j \in \sigma(\Lambda) \\ 0 & \lambda \notin \sigma(\Lambda) \end{cases}\end{aligned}$$

Since every column of Ξ is non-zero, we have the desired conclusion. \square

The two lemmas up next, concern special banded matrices whose construction needs the function below:

$$\begin{aligned} \text{ut} &: \mathbb{C}_\infty \times \mathbb{W} \rightarrow \mathbb{C}_{\infty \times \infty} \\ 0 \leq j &\leq \#\nu \\ \implies \text{ut}[\nu, j] &:= [\text{coeffs}_{\#\nu}[[\nu_i]_{i=1}^{j-1+k}]_{k=1}^{\#\nu-j+1}] \end{aligned}$$

For instance, recall that $\nu_1 = [1 \ 1]^H$. With the definition of ut , we can generate banded matrices of varying sizes, all sampled from the output for $j = 0$:

$$\begin{aligned} \text{ut}[\nu_1, 0] &= \begin{bmatrix} \text{coeffs}_2[\{\}] & \text{coeffs}_2[[1]] & \text{coeffs}_2[[1 \ 1]^H] \end{bmatrix} \\ &= \begin{bmatrix} 1 & -1 & 1 \\ 0 & 1 & -2 \\ 0 & 0 & 1 \end{bmatrix} \\ \text{ut}[\nu_1, 1] &= \begin{bmatrix} -1 & 1 \\ 1 & -2 \\ 0 & 1 \end{bmatrix}, \quad \text{ut}[\nu_1, 2] = \begin{bmatrix} 1 \\ -2 \\ 1 \end{bmatrix} \end{aligned}$$

Generally, we see that

$$(D.1) \quad \begin{aligned} &\text{ut}[\nu, j] \text{ is always full column rank} \\ \therefore &\text{ut}[\nu, 0] \text{ is invertible} \end{aligned}$$

LEMMA D.3.

$$\begin{aligned} D^* &:= \begin{bmatrix} \text{ut}[[\lambda_j]_{j=1}^{r-1}, 0] \\ \mathbf{0}_{(n+1-r) \times r} \end{bmatrix} \\ \implies \Theta D^* &\text{ is invertible.} \end{aligned}$$

Proof.

$$\begin{aligned} \Theta D^* &= \begin{bmatrix} 1 & \lambda_1 & \lambda_1^2 & \cdots & \lambda_1^{r-1} \\ 1 & \lambda_2 & \lambda_2^2 & \cdots & \lambda_2^{r-1} \\ \vdots & \vdots & \vdots & \ddots & \vdots \\ 1 & \lambda_r & \lambda_r^2 & \cdots & \lambda_r^{r-1} \end{bmatrix} \text{ut}[[\lambda_j]_{j=1}^{r-1}, 0] \\ \implies (\Theta D^*)_{ij} &= \text{gp}_r[\lambda_i]^T \text{coeffs}_{r-1}[[\lambda_k]_{k=1}^{j-1}] \\ &= \begin{cases} \prod_{k=1}^{j-1} (\lambda_i - \lambda_k) & j > 1 \\ 1 & j = 1 \end{cases} \end{aligned}$$

In particular, ΘD^* is lower triangular with a non-zero diagonal. Hence, it is invertible. \square

LEMMA D.4.

$$n \geq r \implies \text{ut}[\text{roots}[\text{poly}_{\alpha^*} \text{poly}_{e_{n-r+1}}], 0] = [D^* \ A^*]$$

Proof.

$$\begin{aligned} \nu &:= \text{roots}[\text{poly}_{\alpha^*} \text{poly}_{e_{n-r+1}}] \\ &= \begin{cases} \lambda_i & 1 \leq i \leq r \\ 0 & r < i \leq n \end{cases} \end{aligned}$$

The left hand side (LHS) is a square matrix of dimension $n + 1$. From the definition of ut , we have:

$$\text{LHS}_k = \text{coeffs}_n[[\nu_i]_{i=1}^{k-1}]$$

$$1 \leq k \leq r$$

$$\begin{aligned} \text{LHS}_k &= \begin{bmatrix} \text{coeffs}[[\nu_i]_{i=1}^{k-1}] \\ \mathbf{0}_{n+1-k} \end{bmatrix} \\ &= \begin{bmatrix} \text{coeffs}[[\lambda_i]_{i=1}^{k-1}] \\ \mathbf{0}_{n+1-k} \end{bmatrix} \\ &= \begin{bmatrix} \text{coeffs}[[\lambda_i]_{i=1}^{k-1}] \\ \mathbf{0}_{r-k} \\ \mathbf{0}_{n+1-r} \end{bmatrix} \\ &= \begin{bmatrix} \text{coeffs}_{r-1}[[\lambda_i]_{i=1}^{k-1}] \\ \mathbf{0}_{n+1-r} \end{bmatrix} \\ &= (D^*)_k \end{aligned}$$

$$r + 1 \leq k \leq n + 1$$

$$\begin{aligned} \text{LHS}_k &= \text{poly2coeff}_n \left[\text{poly}_{\text{coeffs}[[\nu_i]_{i=1}^{k-1}]} \right] \\ &= \text{poly2coeff}_n \left[\text{poly}_{\text{coeffs}[[\nu_i]_{i=1}^r]} \text{poly}_{\text{coeffs}[[\nu_i]_{i=r+1}^{k-1}]} \right] \\ &= \text{poly2coeff}_n \left[\text{poly}_{\alpha^*} \text{poly}_{e_{k-r}} \right] \\ &= (A^*)_{k-r} \quad \square \end{aligned}$$

Rationalizing the use of DMD mode norm to discern spurious eigenvalues begins with a coordinate change composed of the above linear transforms.

Proof of Theorem 5.1. Pick any $c \in \mathbb{C}^n$. Using Lemma D.4 and (D.1), we see that $[D^*|A^*]$ is an invertible matrix. This suggests the following change of coordinates:

$$\begin{aligned} \begin{bmatrix} c \\ -1 \end{bmatrix} &=: [D^* \mid A^*] \begin{bmatrix} \tilde{c}_1 \\ \tilde{c}_2 \\ -1 \end{bmatrix} \\ \tilde{c} &:= \begin{bmatrix} \tilde{c}_1 \\ \tilde{c}_2 \end{bmatrix} \\ \tilde{c} \in \mathbb{C}^n \quad \tilde{c}_1 \in \mathbb{C}^r, \quad \tilde{c}_2 \in \mathbb{C}^{n-r} \end{aligned}$$

$$\begin{aligned} \check{\Theta} \begin{bmatrix} c \\ -1 \end{bmatrix} &= \check{\Theta} [D^* \mid A^*] \begin{bmatrix} \tilde{c}_1 \\ \tilde{c}_2 \\ -1 \end{bmatrix} \\ &= \check{\Theta} D^* \tilde{c}_1 \quad (\text{Theorem D.1}) \end{aligned}$$

\check{C} is full column rank & ΘD^* is invertible (Lemma D.3)

$$\begin{aligned}
\therefore \check{C}\Theta \begin{bmatrix} c \\ -1 \end{bmatrix} = 0 &\iff \tilde{c}_1 = 0 \\
\implies \begin{bmatrix} \check{c}^* \\ -1 \end{bmatrix} &= [D^* \mid A^*] \begin{bmatrix} \mathbf{0} \\ \tilde{c}_2^* \\ -1 \end{bmatrix} \\
&= A^* \begin{bmatrix} \tilde{c}_2^* \\ -1 \end{bmatrix} \\
&= \text{band}[\alpha^*, n-r+1] \begin{bmatrix} \tilde{c}_2^* \\ -1 \end{bmatrix} \\
\implies \text{poly} \begin{bmatrix} \check{c}^* \\ -1 \end{bmatrix} &= \text{poly}_{\alpha^*} \text{poly} \begin{bmatrix} \tilde{c}_2^* \\ -1 \end{bmatrix} \quad (\text{Lemma C.2}) \\
\implies \text{roots} \left[\begin{bmatrix} \check{c}^* \\ -1 \end{bmatrix} \right] &\stackrel{\Pi}{=} \begin{bmatrix} \text{roots}[\alpha^*] \\ \text{roots} \left[\begin{bmatrix} \tilde{c}_2^* \\ -1 \end{bmatrix} \right] \end{bmatrix}
\end{aligned}$$

$$\begin{aligned}
&\lambda \in \sigma(\Lambda) \\
&\implies \lambda \in \text{roots}[\alpha^*] \\
&\implies \lambda \in \text{roots} \left[\begin{bmatrix} \check{c}^* \\ -1 \end{bmatrix} \right] \\
&\implies \lambda \in \sigma(\check{T}^*)
\end{aligned}$$

Hence, $\sigma(\Lambda) \subset \sigma(\check{T}^*)$. Since \check{C} is full column rank, we can now apply Lemma D.2 with $\Xi \rightarrow \check{C}$, $\Theta \rightarrow \Theta_{1:-2}$ & $T \rightarrow \check{T}^*$. This shows that the only non-zero DMD modes are those corresponding to the true DMD eigenvalues. \square

Appendix E. Extending mode-norm certification to mean-subtracted data.

Every key result is preceded by a technicality that ensures Lemma D.2 can be applied.

E.1. No preprocessing. Rewriting known objects using the additional notation in Appendix A.

$$\begin{aligned}
Z_{ms}^\lambda &= Z_{\text{msub}_{n+1}}[\lambda] \\
&= C\Theta_{\text{msub}_{n+1}}[\lambda] \\
&= C_{\text{pre}_{n+1}}[\lambda]\tilde{\Theta} \\
X_{ms}^\lambda &= (Z_{ms}^\lambda)_{1:-2}
\end{aligned}$$

In Case 1, removing the mean with respect to λ eliminates the relevant Koopman mode.

LEMMA E.1.

$$C_{red} := \begin{cases} C & \lambda \notin \sigma(\Lambda) \\ \sum_{j=1, \lambda_j \neq \lambda}^r c_j e_j^T & \lambda \in \sigma(\Lambda) \end{cases}$$

$$\Theta_{red} := \begin{cases} \Theta & \lambda \notin \sigma(\Lambda) \\ \sum_{j=1, \lambda_j \neq \lambda}^r e_j \text{gp}_{n+1}[\lambda_j]^T & \lambda \in \sigma(\Lambda) \end{cases}$$

$$r \geq 2 \quad \& \quad \text{Case 1} \implies Z_{ms}^\lambda = C_{red} \Theta_{red}$$

Proof. For Case 1, we have:

$$\zeta_\lambda = \begin{cases} \mathbf{0}_r & \lambda \notin \sigma(\Lambda) \\ e_j & \lambda = \lambda_j \end{cases}$$

Since $Z_{ms}^\lambda = C \Theta \text{msub}_{n+1}[\lambda]$, we can use [Lemma B.1](#) to get the stated relationship. \square

Since Z_{ms}^λ is still a matrix product with a Vandermonde matrix, [Theorem 5.1](#) can be readily applied.

Proof of Theorem 5.3. Case 1 and $r \geq 2 \implies Z_{ms}^\lambda = C_{red} \Theta_{red}$ ([Lemma E.1](#)). By [\(3.17\)](#), \tilde{C} is full column rank $\implies C$ has full column rank. This, in turn, means C_{red} also has full column rank. With $\tilde{C} \rightarrow C_{red}$ and $\Theta \rightarrow \Theta_{red}$, apply [Theorem 5.1](#) to show the numerical spectrum is the truth sans λ . \square

E.2. With pre-processing.

E.2.1. Preserve. In order to talk about $\sigma_{nontriv}[Z_{ms}^\lambda, c_{\lambda, pres}^*]$, we will use the following result:

LEMMA E.2. *Every column of $\text{pre}_{n+1}[\lambda]$ is non-zero if the following hold:*

- $r \geq 2$
- *Case 2*

Proof.

$$\begin{aligned} \zeta_\lambda &= \Theta \frac{\text{gp}_{n+1}[\lambda^{-1}]}{n+1} \\ &= \sum_{j=1}^r e_j \frac{\text{gp}_{n+1}[\lambda_j]^T \text{gp}_{n+1}[\lambda^{-1}]}{n+1} \\ \frac{\text{gp}_{n+1}[\lambda_j]^T \text{gp}_{n+1}[\lambda^{-1}]}{n+1} &= \begin{cases} \left(\frac{(\lambda_j/\lambda)^{n+1}-1}{(\lambda_j/\lambda)-1} \right) \frac{1}{n+1} & \lambda \neq \lambda_j \\ 1 & \lambda = \lambda_j \end{cases} \end{aligned}$$

When λ matches none of λ_j , we only need check if ζ_λ is non-zero. This is indeed true by the second assumption. On the other-hand, when we do have such a match with say λ_i , $r \geq 2$ ensures $e_i - \zeta_\lambda \neq 0$. Combining this with the definition of $\text{pre}_{n+1}[\lambda]$, we get the desired conclusion. \square

We now show that a good dictionary coupled with a minimum number of snapshots can at-least extract $\sigma(\Lambda) - \{\lambda\}$.

Proof of Theorem 5.4. First, we parametrize the constraint set to get an ordinary least squares problem. In order to optimize over the monic polynomials that have λ as a root, we use [Lemma C.2](#).

$$\begin{aligned}
\begin{bmatrix} c \\ -1 \end{bmatrix} &=: \text{band}[\begin{bmatrix} -\lambda & 1 \end{bmatrix}^T, n] \begin{bmatrix} \tilde{c} \\ -1 \end{bmatrix} \\
Z_{ms}^\lambda \begin{bmatrix} c \\ -1 \end{bmatrix} & \\
&= C\Theta \text{msub}_{n+1}[\lambda] \begin{bmatrix} c \\ -1 \end{bmatrix} \\
&= C\Theta \text{msub}_{n+1}[\lambda] \text{band}[\begin{bmatrix} -\lambda & 1 \end{bmatrix}^T, n] \begin{bmatrix} \tilde{c} \\ -1 \end{bmatrix} \\
&= C\Theta \text{band}[\begin{bmatrix} -\lambda & 1 \end{bmatrix}^T, n] \begin{bmatrix} \tilde{c} \\ -1 \end{bmatrix}
\end{aligned}$$

The structure of $\text{band}[\begin{bmatrix} -\lambda & 1 \end{bmatrix}^T, n]$ allows for the last step.

$$\begin{aligned}
(\Theta \text{band}[\begin{bmatrix} -\lambda & 1 \end{bmatrix}^T, n])_{ij} &= \lambda_i^{j-1}(\lambda_i - \lambda) \\
\implies (\Theta \text{band}[\begin{bmatrix} -\lambda & 1 \end{bmatrix}^T, n]) &= (\Lambda - \lambda I_r)\Theta_1 \\
&\implies Z_{ms}^\lambda \begin{bmatrix} c \\ -1 \end{bmatrix} = C(\Lambda - \lambda I_r)\Theta_1 \begin{bmatrix} \tilde{c} \\ -1 \end{bmatrix} \\
&\quad \hat{c}^* := c^*[C(\Lambda - \lambda I_r)\Theta_1] \\
&\implies \begin{bmatrix} c_{\lambda, pres}^* \\ -1 \end{bmatrix} = \text{band}[\begin{bmatrix} -\lambda & 1 \end{bmatrix}^T, n] \begin{bmatrix} \hat{c}^* \\ -1 \end{bmatrix}
\end{aligned}$$

Regardless of whether λ matches any of the λ_j or not, we can apply [Theorem 5.1](#)¹⁶. Hence,

$$\begin{aligned}
\sigma(\Lambda) - \{\lambda\} &\subset \text{roots} \begin{bmatrix} \hat{c}^* \\ -1 \end{bmatrix} \\
\implies \{\lambda\} \cup \sigma(\Lambda) &\subset \text{roots} \begin{bmatrix} c_{\lambda, pres}^* \\ -1 \end{bmatrix} \quad (\text{Lemma C.2})
\end{aligned}$$

To analyse the modes, we note:

$$\begin{aligned}
X_{ms}^\lambda &= (C\Theta \text{msub}_{n+1}[\lambda])_{1:-2} \\
&= (C\text{pre}_{n+1}[\lambda]\tilde{\Theta})_{1:-2} \quad (\text{Lemma B.1}) \\
&= C\text{pre}_{n+1}[\lambda]\tilde{\Theta}_1
\end{aligned}$$

Case 2: Conditions of [Lemma E.2](#) ensure that $C\text{pre}_{n+1}[\lambda]$ has non-zero columns. Apply [Lemma D.2](#) with $\Xi \rightarrow C\text{pre}_{n+1}[\lambda], \Theta \rightarrow \tilde{\Theta}_1 \& T \rightarrow T_{\lambda, pres}^*$.

Case 1: By [Lemma E.1](#), $X_{ms}^\lambda = C_{red}(\Theta_{red})_1$. Apply [Lemma D.2](#) with $\Xi \rightarrow C_{red}, \Theta \rightarrow (\Theta_{red})_1 \& T \rightarrow T_{\lambda, pres}^*$.

□

¹⁶ $C(\Lambda - \lambda I_r)\Theta_1$ will differ, but $n \geq r + 1$ covers both cases

E.2.2. Delay.

$$\begin{aligned}
Z_{ms,del}^\lambda &= \begin{bmatrix} (Z_{ms}^\lambda)_{1:-2} \\ (Z_{ms}^\lambda)_{2:-1} \end{bmatrix} \\
&= \begin{bmatrix} C_{\text{pre}_{n+1}[\lambda]} \\ C_{\text{pre}_{n+1}[\lambda]\tilde{\Lambda}} \end{bmatrix} \tilde{\Theta}_1 \\
&= C_{del} \tilde{\Theta}_1 \\
\tilde{\Lambda} &:= \begin{cases} \begin{bmatrix} \Lambda & \\ & \lambda \end{bmatrix} & \lambda \notin \sigma(\Lambda) \\ \Lambda & \lambda \in \sigma(\Lambda) \end{cases}
\end{aligned}$$

We ensure the new set of observables is Koopman invariant with the following lemma:

LEMMA E.3. *The following conditions are sufficient to ensure C_{del} has full column rank.*

- C is full column rank
- Case 2
- $r \geq 2$

Proof. Proof by contradiction. Suppose we have $v \neq 0 \in \mathcal{N}(C_{del})$. Then,

$$\begin{aligned}
&\begin{bmatrix} C_{\text{pre}_{n+1}[\lambda]} \\ C_{\text{pre}_{n+1}[\lambda]\tilde{\Lambda}} \end{bmatrix} v = 0 \\
\implies &\begin{bmatrix} \text{pre}_{n+1}[\lambda] \\ \text{pre}_{n+1}[\lambda]\tilde{\Lambda} \end{bmatrix} v = 0 \quad (C \text{ is full column rank})
\end{aligned}$$

$\text{pre}_{n+1}[\lambda]$ always has a 1-dimensional nullspace. Hence,

$$\begin{aligned}
&\tilde{\Lambda}v = \beta v \\
\implies &\beta \in \sigma(\Lambda) \cup \{\lambda\} \text{ \& } v = e_\beta
\end{aligned}$$

This means pre_{n+1} has a column of zeroes, which is a contradiction to [Lemma E.2](#). Thus, C_{del} must have full column rank. \square

Finally, we show that $\sigma(\Lambda)$ can be extracted from mean-subtracted-then-delayed data:

Proof of Theorem 5.5. Case 1:

$$\begin{aligned}
Z_{ms}^\lambda &= C_{red}\Theta_{red} && \text{(Lemma E.1)} \\
\implies Z_{ms,del}^\lambda &= \begin{bmatrix} C_{red} \\ C_{red}\Lambda_{red} \end{bmatrix} (\Theta_{red})_{1:-2} \\
&=: C_{red,del}(\Theta_{red})_1
\end{aligned}$$

C is full column rank. So, $C_{red,del}$ also has full column rank. Using [Theorem 5.1](#) with $\check{C} \rightarrow C_{red,del}$ and $\Theta \rightarrow (\Theta_{red})_1$, we can show the numerical spectrum is once again the truth without λ . This is possible since the rows of $(\Theta_{red})_1$ are only composed of the elements of $\sigma(\Lambda) - \{\lambda\}$.

Case 2:

$$Z_{ms,del}^\lambda = C_{del}\tilde{\Theta}_1$$

By [Lemma E.3](#), C_{del} has full column rank. Since $\tilde{\Theta}_1$ has atmost $r + 1$ rows and $n \geq r + 2$, we can apply [Theorem 5.1](#) with $\tilde{C} \rightarrow C_{del}$ and $\Theta \rightarrow \tilde{\Theta}_1$. This completes the proof as $\tilde{\Theta}$ is made using all elements of $\sigma(\Lambda) \cup \{\lambda\}$. \square

Appendix F. Some computational aspects.

F.1. Justifying the numerical checks viz. (6.3). Firstly,

$$(6.3) \implies \sigma(T[c]) \supset B$$

This can be numerically checked with the following indicator of set inclusion:

$$(F.1) \quad \begin{aligned} & \rho_{subset} : \wp(\mathbb{C}) \times \wp(\mathbb{C}) \rightarrow [0, \infty) \\ & \#(B_1), \#(B_2) < \infty \\ \implies & \rho_{subset}[B_1, B_2] := \max_{b_1 \in B_1} \min_{b_2 \in B_2} |b_1 - b_2| \end{aligned}$$

Note that $\rho_{subset}[B_1, B_2] \geq 0$ & $\rho_{subset}[B_1, B_2] = 0 \iff B_1 \subset B_2$. Hence, $\rho_{subset}(B, \sigma(T[c])) < 1$ is equivalent to $\sigma(T[c])$ effectively containing B . Once this is seen to hold, we need to identify elements of $\sigma(T[c])$ with B to compute the relevant $\sigma_{nontriv}$. In lieu of a matching problem, we find the ‘‘closest’’ Companion matrix that contains B up to machine precision.

$$(F.2) \quad \begin{aligned} & c_{Superset}^*, \sigma_{Superset}^* : \wp(\mathbb{C}) \times \mathbb{C}_\infty \rightarrow \mathbb{C}_\infty \\ & c_{Superset}^*[B, c] := \begin{cases} \begin{aligned} & \arg \min_\gamma \|c - \gamma\|_2^2 & \#[c] > \#[B] \\ & \text{subject to} \\ & \sigma(T[\gamma]) \supset B \end{aligned} \\ \text{roots} \circ \begin{bmatrix} c_{Superset}^*[B, c] \\ -1 \end{bmatrix} = B & \text{Otherwise} \end{cases} \\ & \sigma_{Superset}^*[B, c] := \sigma(T[c_{Superset}^*[B, c]]) \end{aligned}$$

In other words, we find the monic polynomial closest to $\text{poly} \begin{bmatrix} -c \\ 1 \end{bmatrix}$ whose roots subsume B . Using [Lemma C.2](#), the above minimization can be cast as a least squares regression.

$$\begin{aligned} & \sigma(T[\gamma]) \supset B \\ \iff & \text{roots} \circ \begin{bmatrix} \gamma \\ -1 \end{bmatrix} \supset B \\ \iff & \exists \beta \text{ such that} & (\text{Lemma C.2}) \\ & \text{poly} \begin{bmatrix} \gamma \\ -1 \end{bmatrix} = \text{poly}_{\text{coeffs}[B]} \text{poly} \begin{bmatrix} \beta \\ -1 \end{bmatrix} \\ \iff & \exists \beta \text{ such that} \\ & \begin{bmatrix} \gamma \\ -1 \end{bmatrix} = \text{band}[\text{coeffs}[B], \#[\gamma] - \#[B] + 1] \begin{bmatrix} \beta \\ -1 \end{bmatrix} \end{aligned}$$

Now, we compute the relative contribution of DMD eigenvalues excluded from B using $\delta_{trivial}$:

$$(F.3) \quad \begin{aligned} & \delta_{trivial} : \mathbb{C}_{\infty \times \infty} \times \wp(\mathbb{C}) \times \wp(\mathbb{C}) \times \mathbb{C}_{\infty} \rightarrow [0, 1] \\ & \delta_{trivial}[Z, B_0, B, c] := 1 - \left(\frac{\sum_{\lambda \in B} \|Xv_{\lambda}\|^2}{\sum_{\lambda \in \sigma_{\mathcal{S}^*_{superset}[B_0, c]}} \|Xv_{\lambda}\|^2} \right) \end{aligned}$$

where $B_0 \supset B$.¹⁷ Hence, whenever (6.3) holds, $\delta_{trivial}$ will be 0. Proving (6.3) for the relevant theorems is now a straightforward algebraic exercise.

F.2. Developing Algorithm 6.1. We are given the results of Companion DMD on N trajectories, all with the same model order \hat{n} . Suppose there is an underlying Koopman invariant subspace of dimension $\hat{r} \leq \hat{n}$, and we want to compute the corresponding Koopman eigenvalues ($\sigma(\Lambda)$). If sufficient delays were taken, Corollary 5.2 says $\forall \lambda \in \sigma(\Lambda)$ and $j \leq N$, $poly_{a_j}[\lambda] = 0$. Thus, Koopman eigenvalues are contained by the optima of the following minimization routine:

$$(F.4) \quad \begin{aligned} & \rho_{SoS} : \mathbb{C}_{\infty \times \infty} \times \mathbb{C}_{\infty} \times \mathbb{C} \rightarrow [0, \infty) \\ & \rho_{SoS}[A, w, \lambda] := \|\text{poly}_{a_j}[\lambda]w_j\|_{j=1}^N \|_2 \\ & \quad = \|\text{gp}_{n+1}[\lambda]^T AW\|_2 \\ & \lambda_{SoS}^* := \arg \min_{\lambda} \rho_{SoS}[A, w, \lambda] \end{aligned}$$

Here, W is a weight matrix that permits accounting for the reliability of c_i . We use $w_i = \frac{1}{1 + \kappa_i \sigma_{tail, i}}$, where κ_i is the condition number of $X_{reduced}$ and $\sigma_{tail, i}$ is the largest singular value of X that was dropped.

When the non-negative function $\rho_{SoS}[A, w, \lambda]$ is known to have a root, i.e. attains the lowest possible value 0, the leading left singular vector of AW can hasten the search for λ_{SoS}^* .

THEOREM F.1. *Suppose the AW is of rank r , and its SVD reads thus:*

$$AW = \sum_{i=1}^r \sigma_i u_i v_i^H$$

Then,

$$\rho_{SoS}[A, w, \lambda_{SoS}^*] = 0 \implies poly_{u_1}[\lambda_{SoS}^*] = 0$$

Proof.

$$\begin{aligned} & \rho_{SoS}[A, w, \lambda^*] = 0 \\ & \iff \text{gp}_{n+1}[\lambda^*]^T AW = 0 \\ & \iff \forall i = 1, \dots, r, \text{gp}_{n+1}[\lambda^*]^T u_i = 0 \\ & \iff \forall i = 1, \dots, r, \text{poly}_{u_i}[\lambda^*] = 0 \\ & \implies \text{poly}_{u_1}[\lambda^*] = 0 \quad \square \end{aligned}$$

In other words, the roots of $poly_{u_1}$ contain all the optima of (F.4), which in-turn subsume the Koopman eigenvalues. In practice, the roots of $poly_{u_1}$ corresponding to the \hat{r} -lowest values of ρ_{SoS} are taken as the estimate of $\sigma(\Lambda)$.

¹⁷When $B_0 = B$, the dependence on B_0 will be dropped for brevity.

REFERENCES

- [1] H. ARBABI AND I. MEZIC, *Ergodic theory, dynamic mode decomposition, and computation of spectral properties of the koopman operator*, SIAM Journal on Applied Dynamical Systems, 16 (2017), pp. 2096–2126.
- [2] H. ARBABI AND I. MEZIC, *Study of dynamics in post-transient flows using koopman mode decomposition*, Physical Review Fluids, 2 (2017), p. 124402.
- [3] H. ARBABI AND I. MEZIC, *Spectral analysis of mixing in 2d high-reynolds flows*, arXiv preprint arXiv:1903.10044, (2019).
- [4] A. AVILA AND I. MEZIC, *Data-driven analysis and forecasting of highway traffic dynamics*, Nature communications, 11 (2020), pp. 1–16.
- [5] B. W. BRUNTON, L. A. JOHNSON, J. G. OJEMANN, AND J. N. KUTZ, *Extracting spatial–temporal coherent patterns in large-scale neural recordings using dynamic mode decomposition*, Journal of neuroscience methods, 258 (2016), pp. 1–15.
- [6] S. L. BRUNTON, B. W. BRUNTON, J. L. PROCTOR, E. KAISER, AND J. N. KUTZ, *Chaos as an intermittently forced linear system*, Nature communications, 8 (2017), pp. 1–9.
- [7] K. K. CHEN, J. H. TU, AND C. W. ROWLEY, *Variants of dynamic mode decomposition: Boundary condition, koopman, and fourier analyses*, Journal of Nonlinear Science, 22 (2012), pp. 887–915.
- [8] R. M. CORLESS, P. M. GIANNI, B. M. TRAGER, AND S. M. WATT, *The singular value decomposition for polynomial systems*, in Proceedings of the 1995 international symposium on Symbolic and algebraic computation, 1995, pp. 195–207.
- [9] M. DELLNITZ AND O. JUNGE, *On the approximation of complicated dynamical behavior*, SIAM Journal on Numerical Analysis, 36 (1999), pp. 491–515.
- [10] Z. DRMAC, I. MEZIC, AND R. MOHR, *Data driven koopman spectral analysis in vandermonde–cauchy form via the dft: Numerical method and theoretical insights*, SIAM Journal on Scientific Computing, 41 (2019), pp. A3118–A3151.
- [11] D. A. HAGGERTY, M. J. BANKS, P. C. CURTIS, I. MEZIC, AND E. W. HAWKES, *Modeling, reduction, and control of a helically actuated inertial soft robotic arm via the koopman operator*, arXiv preprint arXiv:2011.07939, (2020).
- [12] J. P. HESPANHA, *Linear systems theory*, Princeton university press, 2018.
- [13] S. M. HIRSH, K. D. HARRIS, J. N. KUTZ, AND B. W. BRUNTON, *Centering data improves the dynamic mode decomposition*, arXiv preprint arXiv:1906.05973, (2019).
- [14] B. O. KOOPMAN, *Hamiltonian systems and transformation in hilbert space*, Proceedings of the National Academy of Sciences of the United States of America, 17 (1931), p. 315.
- [15] M. KORDA AND I. MEZIC, *Linear predictors for nonlinear dynamical systems: Koopman operator meets model predictive control*, Automatica, 93 (2018), pp. 149–160.
- [16] M. KORDA AND I. MEZIC, *On convergence of extended dynamic mode decomposition to the koopman operator*, Journal of Nonlinear Science, 28 (2018), pp. 687–710.
- [17] J. N. KUTZ, S. L. BRUNTON, B. W. BRUNTON, AND J. L. PROCTOR, *Dynamic mode decomposition: data-driven modeling of complex systems*, SIAM, 2016.
- [18] S. LE CLAINCHE AND J. M. VEGA, *Higher order dynamic mode decomposition*, SIAM Journal on Applied Dynamical Systems, 16 (2017), pp. 882–925.
- [19] A. MAUROY AND I. MEZIC, *On the use of fourier averages to compute the global isochrons of (quasi) periodic dynamics*, Chaos: An Interdisciplinary Journal of Nonlinear Science, 22 (2012), p. 033112.
- [20] A. MAUROY, I. MEZIC, AND J. MOEHLIS, *Isostables, isochrons, and koopman spectrum for the action–angle representation of stable fixed point dynamics*, Physica D: Nonlinear Phenomena, 261 (2013), pp. 19–30.
- [21] I. MEZIC, *Spectrum of the koopman operator, spectral expansions in functional spaces, and state-space geometry*, Journal of Nonlinear Science, pp. 1–55.
- [22] I. MEZIC, *Spectral properties of dynamical systems, model reduction and decompositions*, Nonlinear Dynamics, 41 (2005), pp. 309–325.
- [23] I. MEZIC, *Analysis of fluid flows via spectral properties of the koopman operator*, Annual Review of Fluid Mechanics, 45 (2013), pp. 357–378.
- [24] I. MEZIC, *On numerical approximations of the koopman operator*, arXiv preprint arXiv:2009.05883, (2020).
- [25] I. MEZIC AND A. BANASZUK, *Comparison of systems with complex behavior: spectral methods*, in Proceedings of the 39th IEEE Conference on Decision and Control (Cat. No. 00CH37187), vol. 2, IEEE, 2000, pp. 1224–1231.
- [26] I. MEZIC AND A. BANASZUK, *Comparison of systems with complex behavior*, Physica D: Nonlinear Phenomena, 197 (2004), pp. 101–133.

- [27] R. MOHR AND I. MEZIĆ, *Construction of eigenfunctions for scalar-type operators via laplace averages with connections to the koopman operator*, arXiv preprint arXiv:1403.6559, (2014).
- [28] J. L. PROCTOR AND P. A. ECKHOFF, *Discovering dynamic patterns from infectious disease data using dynamic mode decomposition*, *International health*, 7 (2015), pp. 139–145.
- [29] C. W. ROWLEY, I. MEZIĆ, S. BAGHERI, P. SCHLATTER, AND D. S. HENNINGSON, *Spectral analysis of nonlinear flows*, *Journal of Fluid Mechanics*, 641 (2009), pp. 115–127.
- [30] J. J. RUSHANAN, *On the vandermonde matrix*, *The American Mathematical Monthly*, 96 (1989), pp. 921–924.
- [31] S. SARMAST, R. DADFAR, R. F. MIKKELSEN, P. SCHLATTER, S. IVANELL, J. N. SØRENSEN, AND D. S. HENNINGSON, *Mutual inductance instability of the tip vortices behind a wind turbine*, *Journal of Fluid Mechanics*, 755 (2014), pp. 705–731.
- [32] P. J. SCHMID, *Dynamic mode decomposition of numerical and experimental data*, *Journal of Fluid Mechanics*, 656 (2010), pp. 5–28.
- [33] J. H. TU, C. W. ROWLEY, D. M. LUCHTENBURG, S. L. BRUNTON, AND J. N. KUTZ, *On dynamic mode decomposition: Theory and applications*, arXiv preprint arXiv:1312.0041, (2013).
- [34] M. O. WILLIAMS, I. G. KEVREKIDIS, AND C. W. ROWLEY, *A data-driven approximation of the koopman operator: Extending dynamic mode decomposition*, *Journal of Nonlinear Science*, 25 (2015), pp. 1307–1346.